Chaotic Communications With Correlator Receivers: Theory and Performance Limits

GÉZA KOLUMBÁN, SENIOR MEMBER, IEEE, MICHAEL PETER KENNEDY, FELLOW, IEEE, ZOLTÁN JÁKÓ, AND GÁBOR KIS

Invited Paper

This paper provides a review of the principles of chaotic digital communications using correlator receivers. Modulation schemes using one and two chaotic basis functions, as well as coherent and noncoherent correlation receivers, are discussed. The performance of differential chaos shift keying (DCSK) in multipath channels is characterized. Results are presented for DCSK with multiuser capability and multiple bits per symbol.

Keywords*—Chaotic communications, chaotic modulation schemes, enhanced DCSK, multipath performance, multiple access capable DCSK, theoretical noise performance.*

I. INTRODUCTION

Over the past decade, much research effort has been devoted to the study of communication using chaotic basis functions. The earliest work, which was inspired by the synchronization results of Pecora and Carroll [1], focused on analog modulation schemes with coherent receivers [2]–[6]. Digital modulation using chaotic basis functions and a coherent receiver was first introduced in 1992 [7] and called chaos shift keying (CSK) [8]. Several other chaotic digital modulation schemes were proposed in the following years [9]–[13]. A survey of the state of the art in 1995 can be found in [14].

A robust noncoherent technique called differential chaos shift keying (DCSK) [15] was introduced in 1996, and later optimized as frequency-modulated DCSK (FM-DCSK) [16]. Since then, the methods of communication theory [17]–[19] and statistical analysis [20]–[23] have been applied to chaotic digital modulation schemes, culminating in the development of chaotic counterparts for conventional modulation schemes, and a theoretical classification and understanding of all known chaotic modulation schemes [24]. The state of the art has been summarized in two recent publications [25], [26].

With the theoretical foundations of chaotic communications now established, and a prototype DCSK system demonstrated [27], current research is addressing several areas: 1) characterization of the multipath performance of DCSK [28]; 2) multiuser access for DCSK [29], [30]; 3) variants of CSK and DCSK with improved data rates [31], [32]; and 4) receiver enhancements to exploit determinism in chaotic digital modulation [33]–[35], amongst others.

It is now possible to make definitive statements about the noise and multipath performances of digital modulation schemes using chaotic basis functions. The aim of this tutorial paper is to present theoretical performance bounds for correlator-based chaotic digital communications schemes, to summarize the performance of some representative schemes relative to these limits, and to highlight the expected best case performance in real applications.

In Section II, we extend the basis function approach to modulation and demodulation using chaotic basis functions and highlight the problem that chaotic basis functions are typically orthogonal only in the mean.

The consequence is the estimation problem which results from an inherent characteristic of chaotic communications systems, namely that the basis functions vary from symbol to symbol, even if the same symbol is transmitted repeatedly, and that only infinitely long chaotic signals are orthogonal. We discuss the estimation problem which, if present, degrades the performance of every chaotic digital modulation scheme and propose a solution to get orthonormal basis functions in Section III.

Manuscript received July 20, 2001; revised December 15, 2001. This work was supported in part by the Hungarian–French Intergovernmental S&T Cooperation Programme 1999–2001 under contract numbers NP-1856/98 and F29/98, and in part by the European Commission under the Open LTR initiative (Esprit Project 31103–INSPECT).

G. Kolumbán, Z. Jákó, and G. Kis are with the Department of Measurement and Information Systems, Budapest University of Technology and Economics, H-1521 Budapest, Hungary (e-mail: kolumban@mit.bme.hu).

M. P. Kennedy is with the Department of Microelectronic Engineering, University College, Cork, Ireland (e-mail: Peter.Kennedy@ucc.ie).

Publisher Item Identifier S 0018-9219(02)05247-7.

The digital chaotic modulation schemes which we consider in this work are analyzed in the context of a receiver model which is described in Section IV.

In Section V, we show that a chaotic modulation scheme with one basis function, referred to as antipodal CSK, can theoretically achieve the noise performance of binary phase-shift keying (BPSK). In practice, this performance cannot be reached because at least two problems must be overcome: the estimation problem and the recovery of basis function from the noisy and modulated received signal. Recovery of chaotic basis functions independently of the modulation is difficult to achieve; failure to solve this problem to date has impeded the development of coherent demodulators for chaotic communications.

With no available solution to the problem of basis function recovery independently of the modulation, alternative modulation schemes have been proposed which exploit two basis functions. In Section VI, we show that CSK with two orthonormal basis functions and a coherent receiver, referred to as chaotic switching, can theoretically achieve the noise performance of coherent frequency-shift keying (FSK). This level of performance can be reached only if the estimation problem is solved and the basis functions can be recovered at the demodulator. While the former problem can be readily solved, implementation difficulties associated with the recovery of chaotic basis functions cause published results for coherent CSK receivers to lag far behind their theoretical noise performance.

Given the difficulty of recovering chaotic basis functions at the receiver, one may ask what is the best performance that can be expected without recovering the basis functions. We will show that the noise performance of CSK with two appropriately constructed basis functions and a differentially coherent correlation receiver is at most 3 dB worse than that of differential phase-shift keying (DPSK) with autocorrelation demodulation [36].

The noise performance and feasibility of chaotic modulation schemes are compared in Section VII. If it is possible to recover the basis function at the receiver independently of the modulation, then antipodal CSK, where one basis function is used, offers the best noise performance of all known chaotic digital modulation schemes.

In practice, the primary issue influencing the choice of a chaotic or conventional basis function in coherent communications is the robustness of the basis function recovery process. The current state of the art is that antipodal CSK has not been demonstrated. The reported performance of CSK with two basis functions lags significantly behind that of coherent FSK, which represents the theoretical upper bound on its performance.

If one considers only the noise performance of the modulation schemes in a band-limited single-ray additive white Gaussian noise (AWGN) channel [37] under propagation conditions where the basis functions can be recovered at the receiver, then higher performance can be achieved by using a conventional narrow-band modulation scheme with periodic, rather than chaotic, basis functions. If it is not possible to recover the chaotic basis functions at the receiver, then, in a single-ray channel, DCSK with differentially coherent detection offers the best noise performance.

Although the noise performance of DCSK lags 3 dB behind that of its conventional narrow-band counterpart (DPSK with autocorrelation demodulation), the performance degradation due to multipath is much less in the DCSK system. Multipath propagation is present in many important applications such as indoor radio, mobile communication and wireless local area networks. The multipath performance of DCSK is discussed in Section VIII.

In a wireless local area network (WLAN), which is one possible application for chaotic communications, at least limited multiple access capability must be offered. To avoid interference among the different users, orthogonal channels have to be developed. A novel solution is discussed in Section IX, where the orthogonality of the DCSK channels is ensured by using Walsh functions.

In FM-DCSK, frequency modulation is introduced to overcome the estimation problem which is a common drawback of proposed chaotic modulation schemes. This modulation scheme with a differentially coherent receiver offers the best noise performance of all published correlation-based chaotic modulation schemes. Unfortunately, even its noise performance lags behind that of DPSK implemented with autocorrelation demodulation.

This drawback can be overcome by using the techniques described in Section X. The simplest enhancement technique improves the noise performance by 1.4 dB, while the improvement of the most advanced technique, which requires a more complex receiver, is 3.4 dB.

II. Chaotic Modulation and Demodulation

Chaotic digital modulation is concerned with mapping symbols to analog chaotic waveforms. In CSK [8], information is carried in the weights of a combination of basis functions which are derived from chaotic signals. Differential chaos shift keying [15] is a variant of CSK where the basis functions have a special structure and the information can be recovered from the correlation between the parts of the basis functions.

In this work, we concentrate on the transmission and reception of a single isolated symbol; problems arising from the reception of symbol streams are not treated here.

A. Modulation

Using the notation introduced in [17], the elements of the CSK signal set are defined by

$$s_m(t) = \sum_{j=1}^{N} s_{mj} g_j(t), \qquad j = 1, 2, \ldots, N$$

where m is the index of the current symbol being transmitted, the weights s_{mj} are the elements of the signal vector, and the basis functions $g_j(t)$ are chaotic waveforms. The signals $s_m(t)$ may be produced conceptually as shown in Fig. 1.

Note that the shape of the basis functions is not fixed in chaotic communications. This is why the signal $s_m(t)$

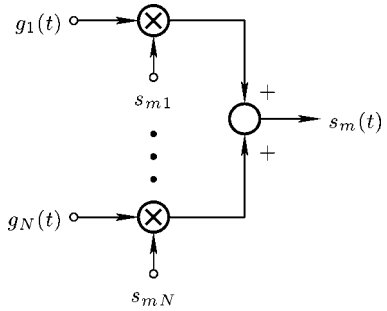

Fig. 1. Generation of the elements of the signal set.

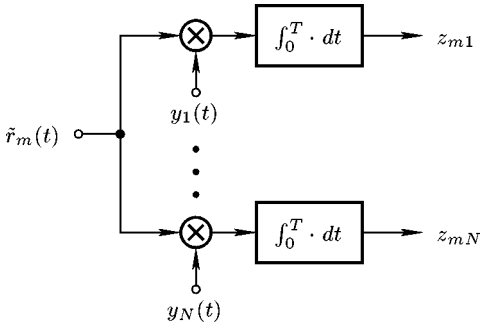

Fig. 2. Determination of the observation signals in a correlation receiver.

which is transmitted through the channel has a different shape during every symbol interval of duration T, even if the same symbol is transmitted repeatedly. As a result, the transmitted signal is never periodic.

To achieve the best noise performance, basis functions must be orthonormal [37]. In the general case, chaotic basis functions are at best orthonormal over an interval of length T only in the mean, i.e.,

$$E\left[\int_T g_j(t)g_k(t)\,dt\right] = \begin{cases} 1, & \text{if } j=k \\ 0, & \text{otherwise} \end{cases} \tag{1}$$

where T is the bit duration and $E[\cdot]$ denotes the expectation operator.[1]

Equation (1) identifies another important characteristic of chaotic modulation schemes: since the basis functions are not fixed waveforms but chaotic signals, they have to be modeled as sample functions of a stochastic process.[2]

Consequently, the cross correlation and autocorrelation of basis functions evaluated for the bit duration become random numbers which can be characterized by their probability distributions, e.g., by their mean value and variance.[3] The consequence of this property, called the *estimation problem*, will be discussed in Section III.

B. Demodulation

Since the shape of the basis functions is not fixed in chaotic communications, the matched filter approach [37] cannot be used for demodulation. However, the message may be recovered at the receiver by correlating the received signal with reference signals $y_1(t)$, $y_2(t)$, ..., $y_N(t)$, and forming the corresponding observation signals z_{m1}, z_{m2}, ..., z_{mN}, as shown in Fig. 2.

The reference signal $y_j(t)$ can be generated in a number of different ways: it can be the received signal itself, or a delayed version of the received signal, or a basis function recovered from the received signal.

In a coherent correlation receiver, the reference signals $y_j(t)$ are locally regenerated copies of the basis functions $g_j(t)$. When signal $s_m(t)$ is transmitted and $y_j(t) = g_j(t)$, the jth element z_{mj} of the observation vector emerging from the jth correlator is given by

$$\begin{aligned} z_{mj} &= \int_0^T s_m(t)y_j(t)\,dt \\ &= \int_0^T \left[\sum_{k=1}^{N} s_{mk}g_k(t)\right] g_j(t)\,dt \\ &= s_{mj}\int_0^T g_j^2(t)\,dt + \sum_{\substack{k=1 \\ k\neq j}}^{N} s_{mk}\int_0^T g_j(t)g_k(t)\,dt \end{aligned}$$

where according to (1) $E[\int_T g_j^2(t)\,dt] = 1$ and $E[\int_T g_j(t)g_k(t)\,dt] = 0$ for $k \neq j$.

If the bit duration T is sufficiently long, then $\int_0^T g_j^2(t)\,dt \approx 1$ and $\int_0^T g_k(t)g_j(t)\,dt \approx 0$. In this case,

$$z_{mj} \approx s_{mj}. \tag{2}$$

Thus, in the case of a distortion- and noise-free channel, and for a sufficiently large bit duration, the observation and signal vectors are approximately equal to each other.

In this way, the elements s_{mj} of the signal vector can be recovered (approximately) by correlating the received signal with the reference signals $y_j(t)$.

In real applications, the elements z_{mj} of the observation vector are random numbers because of the estimation problem and additive channel noise; in addition, their values are influenced by a number of factors including channel filtering and distortion. This is why the observation vector can be considered only as an *estimation* of the signal vector.

The number of wrong decision is determined by the probability distribution of the observation signal. As a rule of thumb, the smaller the variance, the lower the bit error rate (BER). While filtering, distortion, and noise effects are common to all communication systems, the estimation problem is a consequence of using chaotic basis functions. The estimation problem increases the variance of the observation signal and so corrupts the noise performance. In the

[1]We are considering the expectation of $\int_{mT}^{(m+1)T} g_j(t)g_k(t)\,dt$ over all m. Although it is deterministic, the chaotic basis functions $g_j(\cdot)$ are typically different in each successive interval of length T. Note that the expectation operator refers to the average over all intervals. For convenience in the remainder of the paper, we consider each interval $[mT,\ (m+1)T]$ as equivalent to the interval $[0,\ T]$.

[2]In a chaotic stochastic signal model, the ensemble of sample functions is generated by the same chaotic attractor starting from all possible initial conditions [38].

[3]By contrast, for example, sine and cosine basis functions can be made orthonormal by appropriate scaling and by choosing the ratio of the bit duration and half the period of each basis function to be an integer.

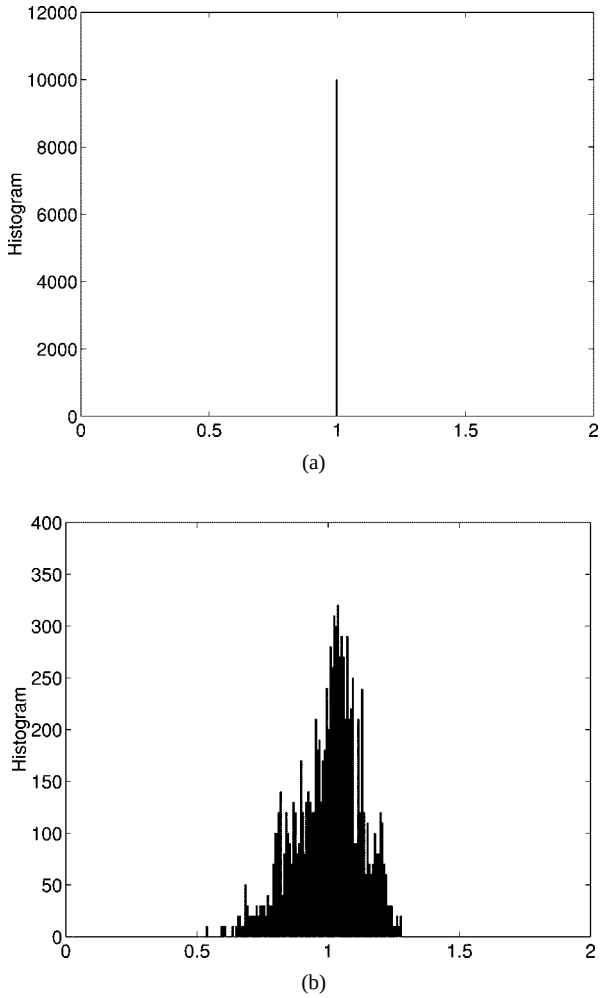

Fig. 3. Samples of $\int_0^T g_j^2(t)dt$ for (a) periodic and (b) chaotic basis functions $g_j(t)$.

next section, we explain the two sources of the estimation problem and indicate how to solve it.

III. Estimation Problem

In a typical conventional modulation scheme, the basis functions are periodic and the bit duration T is an integer multiple of the period of the basis functions; hence, $\int_0^T g_j^2(t)\,dt = 1$ and $\int_0^T g_j(t)g_k(t)\,dt = 0$, i.e., the auto- and cross correlation estimation problems do not appear.

A. The Autocorrelation Estimation Problem

A chaotic basis function $g_j(t)$ is different in every interval of length T. Consequently, $\int_0^T g_j^2(t)\,dt$ is different for every symbol, even if the same symbol is transmitted repeatedly.

Fig. 3(a) and (b) shows histograms of samples of $\int_0^T g_j^2(t)\,dt$ for conventional periodic and chaotic waveforms $g_j(t)$, respectively. In the periodic case, all samples lie at $\int_0^T g_j^2(t)\,dt = 1$. By contrast, the samples in the chaotic case are centered at 1, as before, but have nonzero variance.

This nonzero variance causes the components z_{mj} of the observation vector to differ from the corresponding components s_{mj} of the signal vector, and therefore causes errors

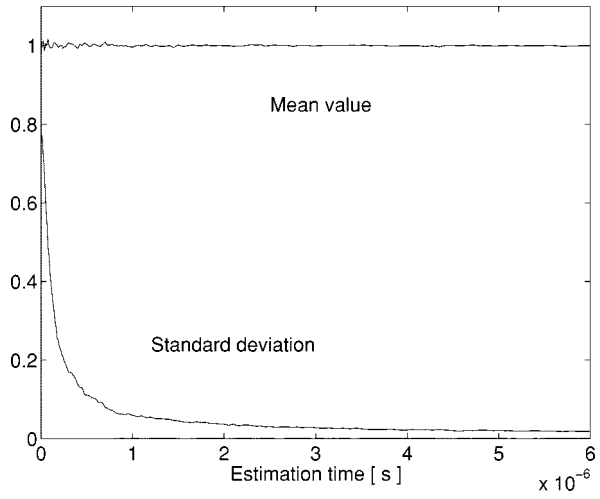

Fig. 4. Mean and standard deviation of the estimation of $\int_0^T g_1^2(t)dt$ versus the estimation time.

in interpreting the received signal, even in the case of a distortion- and noise-free channel. The most significant consequence of nonzero variance is a considerable degradation in noise performance, as will be seen in Figs. 9 and 11 in Section V.

Let the equivalent statistical bandwidth [39] of the chaotic signal $g_j(t)$ be defined by

$$B_{eq} = \frac{1}{S_C(0)} \int_0^\infty S_C(f)\,df$$

for low-pass and by

$$B_{eq} = \frac{1}{2S_C(f_C)} \int_0^\infty S_C(f)\,df$$

for bandpass chaotic basis functions, where $S_C(f)$ is the power spectral density associated with the chaotic stochastic signal model and f_C denotes the center frequency of a bandpass chaotic basis function [38]. Then the standard deviation of samples of $\int_0^T g_j^2(t)\,dt$ scales approximately as $1/(B_{eq}T)$, as shown in Fig. 4. Note that the variance of estimation can be reduced by increasing the statistical bandwidth of the transmitted chaotic signal or by increasing the bit duration T [39]. Alternatively, one may solve the autocorrelation estimation problem directly by modifying the generation of the basis functions such that the transmitted energy for each symbol is kept constant [20].

1) Sample Solution: Use FM: Recall that the instantaneous power of an FM signal does not depend on the modulation, provided that the latter is slowly varying compared to the carrier. Therefore, one way to produce a chaotic sample function with constant energy per bit E_b is to apply a chaotic signal to a frequency modulator; this can be achieved as shown in Fig. 5.

2) Conclusion: A necessary condition for chaotic digital modulation schemes to reach their maximum noise performance is that the chaotic sample functions should have constant energy per bit. Therefore, in the remainder of this paper,

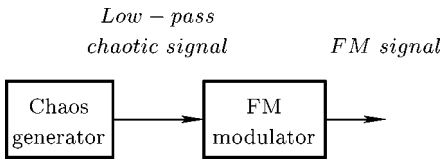

Fig. 5. Block diagram illustrating the generation of chaotic sample functions with constant energy per bit by means of a frequency modulator.

we will assume that the chaotic sample functions have constant E_b. In particular, we normalize the basis functions such that, for all j

$$\int_0^T g_j^2(t)\,dt = 1.$$

B. The Cross Correlation Estimation Problem

The estimation problem also arises when evaluating the cross correlation between different chaotic basis functions of finite length. Although $E[\int_T g_j(t)g_k(t)\,dt] = 0$, $\int_0^T g_j(t)g_k(t)\,dt \neq 0$ in general, unless $g_j(t)$ and $g_k(t)$ are orthogonal in $[0, T]$.

1) Sample Solution: DCSK Basis Functions: Although infinitely long chaotic signals are orthogonal, chaotic sample functions of finite length do not meet the orthogonality requirement of digital telecommunications due to the cross correlation estimation problem. However, orthogonality can be assured by using appropriately constructed basis functions.

For example, orthogonal basis functions can be generated by combining the Walsh functions [40] with chaotic signals.

Define basis functions $g_1(\cdot)$ and $g_2(\cdot)$:

$$g_1(t) = \begin{cases} +\dfrac{1}{\sqrt{E_b}}\,c(t), & 0 \le t < T/2 \\ +\dfrac{1}{\sqrt{E_b}}\,c(t-T/2), & T/2 \le t < T \end{cases}$$

$$g_2(t) = \begin{cases} +\dfrac{1}{\sqrt{E_b}}\,c(t), & 0 \le t < T/2 \\ -\dfrac{1}{\sqrt{E_b}}\,c(t-T/2), & T/2 \le t < T \end{cases} \tag{3}$$

where $c(t)$ is derived from a chaotic waveform.

Each basis function consists of two segments, the first and second called the reference and information-bearing chips, respectively. Because the digital information to be recovered is also carried in the correlation between the reference and information-bearing chips, we call these differential CSK (DCSK) basis functions.

Note that the orthogonality of basis functions is assured by the first two Walsh functions [40]

$$W_1 = [1 \quad 1], \quad \text{and} \quad W_2 = [1 \quad -1].$$

By using Walsh functions, the signal $c(t)$ in (3) may have any shape. The DCSK basis functions $g_1(t)$ and $g_2(t)$ are always orthogonal, i.e., $\int_0^T g_1(t)g_2(t)\,dt = 0$.

Note that, in addition, if $c(t)$ is produced by FM, $\int_0^T g_1^2(t)\,dt = \int_0^T g_2^2(t)\,dt = 1$. Therefore, the FM-DCSK [16] basis functions are *orthonormal*.

2) Conclusion: By using orthogonal basis functions, the cross correlation estimation problem can be solved.

IV. Receiver Model

Noise performance is the most important characteristic of a modulation scheme and receiver configuration. All of the correlator-based chaotic modulation techniques to be discussed in this paper can be considered under the unifying umbrella of the basis function approach. Here, we consider their noise performance, assuming the receiver block diagram shown in Fig. 6, where $r_m(t) = s_m(t) + n(t)$ and $\tilde{s}_m(t)+\tilde{n}(t)$ denote the noisy received signal before and after filtering, respectively. Since the noise performance of noncoherent receivers depends on the bandwidth of the channel (selection) filter, an ideal bandpass filter with a total RF bandwidth of $2B$ is included explicitly in the block diagram.

This model can be used to characterize the performance of noncoherent, differentially coherent, and coherent correlation receivers. The difference between these schemes is primarily due to the way in which the reference signal $y(t)$ is generated at the receiver. A synchronization time $T_S > 0$ has to be considered if the reference signal is recovered by synchronization at the beginning of each symbol.

In the following sections, we use this model to develop performance limits for CSK with one and two basis functions.

V. CSK With One Basis Function

A. Modulation

In the simplest case of binary CSK, a single chaotic basis function $g_1(t)$ is used, i.e.,

$$s_m(t) = s_{m1}g_1(t).$$

Two basic types of CSK based on a single basis function have been proposed: chaotic on–off keying (COOK) [41] and antipodal CSK [42].

In COOK, symbol "1" is represented by $s_1(t) = \sqrt{2E_b}\,g_1(t)$ and symbol "0" is given by $s_2(t) = 0$. Equivalently

$$s_{11} = \sqrt{2E_b}; \qquad s_{21} = 0$$

where E_b denotes the average energy per bit and we have assumed that the probabilities of symbols "1" and "0" are equal.

The upper limit on the noise performance of a modulation scheme is determined by the separation of the message points in the signal space; the greater the separation, the better the noise performance. Fig. 7 shows the signal-space diagram for COOK, where the distance between the message points is $\sqrt{2E_b}$.

In antipodal CSK, symbol "1" is represented by $s_1(t) = \sqrt{E_b}\,g_1(t)$ and symbol "0" is given by $s_2(t) = -\sqrt{E_b}\,g_1(t)$. Fig. 8 shows the signal-space diagram for antipodal CSK.

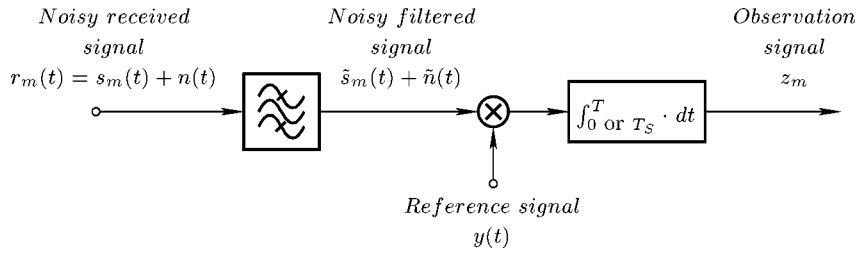

Fig. 6. General block diagram of a digital chaotic communications receiver.

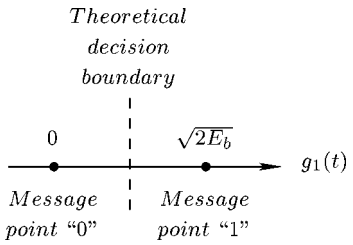

Fig. 7. Signal-space diagram for binary COOK.

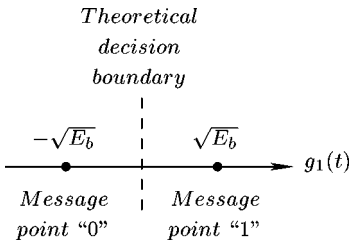

Fig. 8. Signal-space diagram for binary antipodal CSK.

The distance between the message points is $2\sqrt{E_b}$ in this case. Consequently, the noise performance of antipodal CSK is potentially superior to that of COOK.

While the modulator determines the distance between the message points, the noise performance of the system depends on the efficiency with which the demodulator exploits this separation.

In principle, the best noise performance in an AWGN channel can be achieved by using a coherent receiver [36]. In practice, the propagation conditions may be so poor that it is difficult, if not impossible, to regenerate the basis functions at the receiver. Under these conditions, a noncoherent or differentially coherent receiver may offer better performance.

B. Demodulation

1) Coherent Correlation Receiver: In a coherent correlation receiver, the reference signal $y(t)$ at the receiver is the basis function which has been recovered from the noisy filtered received signal. The observation signal is given by

$$\begin{aligned} z_m &= \int_{T_S}^{T} [\tilde{s}_m(t) + \tilde{n}(t)] y(t)\, dt \\ &= \int_{T_S}^{T} [s_{m1}\tilde{g}_1(t) + \tilde{n}(t)] y(t)\, dt \\ &= s_{m1} \int_{T_S}^{T} \tilde{g}_1(t) y(t)\, dt + \int_{T_S}^{T} \tilde{n}(t) y(t)\, dt \end{aligned} \tag{4}$$

where we assume that the synchronization transient lasts at most T_S seconds per symbol period. In the best case, where synchronization of $y(t)$ with $g_1(t)$ is maintained throughout the transmission, $T_S = 0$.

Note that the observation signal z_m is a *random variable* whose mean value depends on the energy per bit of the chaotic signal and the "goodness" with which the basis function has been recovered [see the first term in (4)].

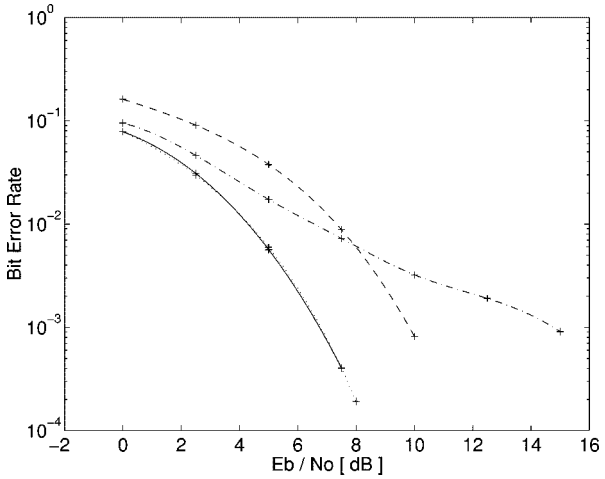

Fig. 9. Simulated optimum noise performance of COOK and antipodal CSK with a coherent correlation receiver: antipodal CSK with constant E_b (solid curve); COOK with equiprobable symbols and constant E_b (dashed curve); antipodal CSK with nonconstant energy per bit (dash–dot curve). Coherent BPSK is shown (dotted curve) for comparison.

In a noise-free channel with exact recovery of the basis function, a sufficiently wide-band channel filter, and permanent synchronization, $y(t) = g_1(t)$, $\tilde{g}_1(t) = g_1(t)$, and $T_S = 0$. The observation variable in this case is

$$z_m = s_{m1} \int_0^T g_1^2(t)\, dt = s_{m1}.$$

Therefore, the coherent correlation receiver can be used to demodulate both COOK and antipodal CSK, provided that the basis function $g_1(t)$ can be recovered from the received signal $s_m(t)$.

The performance of a digital communications system is expressed by the BER [37]. Fig. 9 shows, by simulation, the theoretical upper bounds on the noise performance of coherent COOK and coherent antipodal CSK with one basis function. Note that the noise performance of antipodal CSK

(solid) exceeds that of COOK (dashed) by 3 dB; this is a consequence of the greater separation of the message points (by a factor of $\sqrt{2}$) at the modulator.

If one basis function is used, then only the autocorrelation estimation problem appears. Fig. 9 shows its manifestation for the case of antipodal CSK when the energy per bit has nonzero variance. In this case, the effect of channel noise, characterized by its power spectral density $N_0/2$, is dominated at high E_b/N_0 by the variance of the energy per bit $E_b = \int_0^T g_1^2(t)\,dt$. If $\int_0^T g_1^2(t)\,dt$ is kept constant, the problem disappears.

2) Theoretical Noise Performance of Coherent Antipodal CSK: Assuming constant E_b, the theoretical noise performance for coherent antipodal CSK was reported in [42]

$$\text{BER} = \frac{1}{2}\,\text{erfc}\left(\sqrt{\frac{E_b}{N_0}}\right). \tag{5}$$

As with all conventional coherent modulation schemes, the noise performance does not depend on the bit duration or the RF bandwidth of the channel filter.

The theoretical predictions of (5) are compared with the results of computer simulations [43] in Fig. 10, where the solid curve shows the noise performance predicted by (5), while the results of simulations are denoted by "+" marks.

3) Conclusion: Equation (5) shows that the noise performance of an antipodal CSK modulator and coherent correlation receiver theoretically matches that of BPSK [37]. However, this performance can be achieved only if the following necessary conditions are satisfied:

1) the energy per bit is kept constant;
2) the basis function $g_1(t)$ is recovered exactly at the receiver, independently of the modulation.

The first condition can be satisfied in the case of chaotic basis functions by using FM, for example, as described in Section III.

Although several strategies for recovering the basis function $g_1(t)$ have been proposed in the literature, under the title "chaotic synchronization" [1]–[14], we are not aware of any chaotic synchronization technique which can regenerate the basis function exactly, *independently of the modulation.*[4] If the basis function cannot be recovered exactly, the noise performance of antipodal modulation is degraded significantly.

4) Noncoherent Correlation Receiver: Although antipodal CSK cannot be demodulated without recovering the basis function, COOK can be demodulated by means of a noncoherent receiver.

In a noncoherent correlation receiver, the reference signal $y(t)$ is equal to the noisy filtered signal $\tilde{s}_m(t)+\tilde{n}(t)$, and the observation signal can be expressed as

$$\begin{aligned} z_m &= \int_0^T [\tilde{s}_m(t)+\tilde{n}(t)]^2\,dt \\ &= \int_0^T \tilde{s}_m^2(t)\,dt + 2\int_0^T \tilde{s}_m(t)\tilde{n}(t)\,dt + \int_0^T \tilde{n}^2(t)\,dt \end{aligned}$$

[4]Robustness of chaotic synchronization in the presence of noise has been studied theoretically in [48].

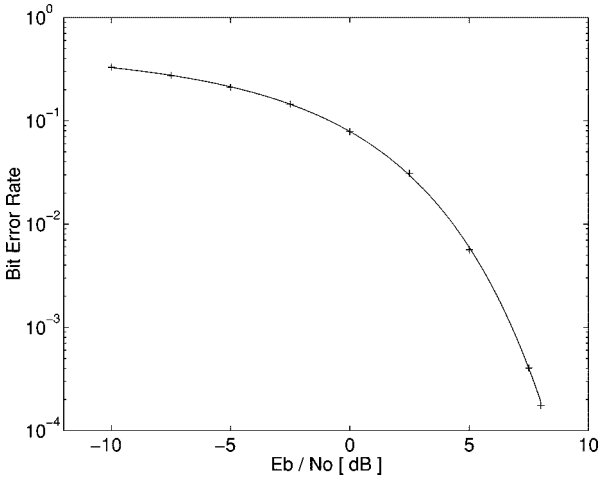

Fig. 10. Comparison between the theoretical (solid curve) and simulated ("+" marks) noise performances of coherent antipodal CSK.

$$\begin{aligned} &= s_{m1}^2\int_0^T \tilde{g}_1^2(t)\,dt + 2s_{m1}\int_0^T \tilde{g}_1(t)\tilde{n}(t)\,dt \\ &\quad + \int_0^T \tilde{n}^2(t)\,dt. \end{aligned} \tag{6}$$

In the noise-free case, if the signal $s_m(t)$ emerges unchanged from the channel [$\tilde{g}_1(t) = g_1(t)$], the observation signal is equal to the energy of the transmitted symbol, i.e.,

$$z_m = s_{m1}^2\int_0^T g_1^2(t)\,dt.$$

Since $s_{11}^2 = s_{21}^2 = E_b$ in antipodal CSK, these symbols cannot be distinguished at the receiver. By contrast, the observation signals z_1 and z_2 of the two COOK symbols differ by $2E_b$, where E_b is the average bit energy.

Due to the last term in (6), the noise performance of noncoherent COOK depends on both the bit duration T and the RF channel bandwidth $2B$. Fig. 11 shows the noise performance for the best case, where $BT = 1$.

Fig. 11 shows that the autocorrelation estimation problem manifests itself if $\int_0^T g_1^2(t)\,dt$ is not constant (see dashed curve) but the problem disappears, as expected, when $\int_0^T g_1^2(t)\,dt$ is kept constant (see solid curve).

The noise performance of noncoherent COOK is worse than that of coherent COOK due to the second and third terms in (6). Although $E[\int_0^T \tilde{g}_1(t)\tilde{n}(t)\,dt] = 0$, $E[\int_0^T \tilde{n}^2(t)\,dt] > 0$. Hence, z_m is a biased estimator of s_{m1}^2 and the decision threshold must be adjusted depending on the signal-to-noise ratio (SNR) measured at the demodulator input.

5) Conclusion: For a given E_b/N_0, a single basis function, and a noncoherent correlation receiver, the best noise performance for a chaotic digital modulation scheme in an AWGN channel can be achieved by COOK. However, COOK suffers two significant drawbacks:

1) the transmitted energy per bit varies between zero for symbol "0" and $2E_b$ for symbol "1";
2) the optimum decision threshold at the receiver depends on the SNR.

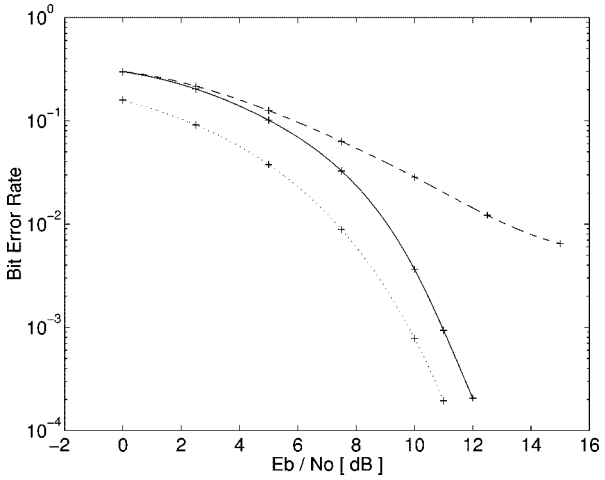

Fig. 11. Simulated noise performance of noncoherent COOK with constant (solid curve) and varying (dashed curve) energy per symbol. Coherent COOK is shown (dotted curve) for comparison.

The design of a digital communications receiver can be simplified considerably if the decision threshold at the demodulator is independent of the SNR. By using two basis functions, this condition can be satisfied.

VI. CSK With Two Basis Functions

A. Modulation

In CSK with two basis functions, the elements of the signal set are given by

$$s_m(t) = s_{m1}g_1(t) + s_{m2}g_2(t)$$

where the basis functions $g_1(t)$ and $g_2(t)$ are derived from chaotic sources.

In a special case of binary CSK [8], also called "chaotic switching" [13], the two elements of the signal set are simply weighted basis functions; the transmitted sample functions are $s_1(t) = \sqrt{E_b}\, g_1(t)$ and $s_2(t) = \sqrt{E_b}\, g_2(t)$, representing symbols "1" and "0," respectively. The corresponding signal vectors are $(s_{11}\ s_{12}) = (\sqrt{E_b}\, 0)$ and $(s_{21}\ s_{22}) = (0\ \sqrt{E_b})$, where E_b denotes the average energy per bit.

The signal-space diagram for chaotic switching and orthonormal basis functions $g_1(t)$ and $g_2(t)$ is shown in Fig. 12. Note that the Euclidean distance between the two message points is $\sqrt{2E_b}$, which is the same as for coherent COOK but is less than that of coherent antipodal CSK. This implies that the noise performance of chaotic switching is at best 3 dB worse than that of the antipodal modulation scheme described in Section V.

B. Demodulation

1) Coherent Correlation Receiver: A coherent correlation receiver, as shown in Fig. 13, may be used to estimate the elements s_{mj} of the signal vector. In the noise-free case, with perfect regeneration of the basis functions, $y_1(t) = g_1(t)$ and $y_2(t) = g_2(t)$.

In the case of chaotic switching with constant E_b, and assuming that the basis functions $g_1(t)$ and $g_2(t)$ are orthonormal in the interval $[0,\ T]$, the outputs of the correlators are obtained as

$$z_{11} = s_{11}\int_0^T g_1^2(t)\,dt = \sqrt{E_b}$$
$$z_{12} = s_{12}\int_0^T g_1(t)g_2(t)\,dt = 0$$

when symbol "1" is transmitted, and

$$z_{21} = s_{21}\int_0^T g_1(t)g_2(t)\,dt = 0$$
$$z_{22} = s_{22}\int_0^T g_2^2(t)\,dt = \sqrt{E_b}$$

when symbol "0" is transmitted.

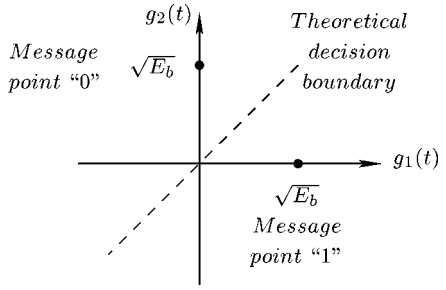

Fig. 12. Signal-space diagram of chaotic switching.

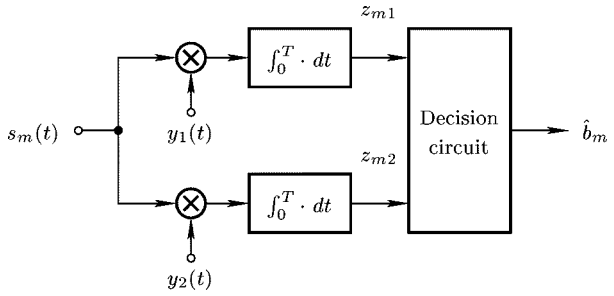

Fig. 13. Idealized coherent correlation receiver for CSK with two basis functions. The effect of the channel filter is neglected.

Thus, the correlation receiver structure may be used to identify which element of the signal set is more likely to have produced the received signal [17]. In particular, if $z_{m1} > z_{m2}$, then the decision circuit decides in favor of symbol "1"; if $z_{m1} < z_{m2}$, then the decision circuit decides in favor of symbol "0."

Consider now the noise performance of chaotic switching with a coherent correlation receiver which also includes the channel filter. In this case, the reference signal in each arm is a regenerated basis function $y_j(t)$ which is derived from the filtered noisy received signal $\tilde{s}_m(t) + \tilde{n}(t)$.

The observation signals z_{mj}, $j = 1,\ 2$, are given by

$$z_{mj} = \int_{T_S}^{T} [\tilde{s}_m(t) + \tilde{n}(t)]y_j(t)\,dt$$
$$= \int_{T_S}^{T} [s_{m1}\tilde{g}_1(t) + s_{m2}\tilde{g}_2(t) + \tilde{n}(t)]y_j(t)\,dt$$

$$= s_{m1} \int_{T_S}^{T} \tilde{g}_1(t) y_j(t)\, dt + s_{m2} \int_{T_S}^{T} \tilde{g}_2(t) y_j(t)\, dt + \int_{T_S}^{T} \tilde{n}(t) y_j(t)\, dt \quad (7)$$

where we assume that the synchronization transient lasts at most T_S seconds per symbol period.

Note that z_{mj} is a *random variable,* whose mean value depends on the energy per bit of the chaotic signal and the "goodness" with which the basis functions have been recovered [see the first two terms in (7)].

At best, $y_j(t) \approx \tilde{g}_j(t) \approx g_j(t)$, and synchronization of $y_j(t)$ with $g_j(t)$ is maintained throughout the transmission, i.e., $T_S = 0$. In this case

$$z_{mj} = s_{m1} \int_{0}^{T} g_1(t) g_j(t)\, dt + s_{m2} \int_{0}^{T} g_2(t) g_j(t)\, dt + \int_{0}^{T} \tilde{n}(t) g_j(t)\, dt. \quad (8)$$

We have seen that the variance of $\int_0^T g_j^2(t)\, dt$ can be reduced to zero by keeping E_b constant. The cross correlations $\int_0^T g_k(t) g_j(t)\, dt$, $k \neq j$ can be zeroed by selecting orthogonal basis functions.

By choosing orthonormal basis functions, such as the DCSK functions described in Section III-B1

$$z_{mj} = s_{mj} + \int_{0}^{T} \tilde{n}(t) g_j(t)\, dt$$

provides an unbiased estimate of s_{mj}.

Fig. 14 shows the simulated upper bound on the noise performance of chaotic switching with two basis functions.

2) Theoretical Noise Performance of Coherent DCSK: Since DCSK provides orthonormal basis functions, it offers the best attainable noise performance over an AWGN channel when CSK with two basis functions is used. The theoretical noise performance of coherent DCSK is equal to that of coherent FSK and is given by [42]

$$\text{BER} = \frac{1}{2} \operatorname{erfc}\left(\sqrt{\frac{E_b}{2N_0}} \right). \quad (9)$$

Note again that the noise performance of coherent receivers depends neither on the bit duration nor on the RF bandwidth of the channel filter.

Fig. 14 shows the noise performance of the coherent DCSK modulation scheme predicted from (9) (solid curve) and determined by computer simulation ("+" marks).

A detailed analysis of the observation signal (4) shows that (9) is also valid for coherent COOK when $T_S = 0$ and E_b is kept constant. Comparison of (5) and (9) shows that the noise performance of coherent COOK and DCSK lags 3 dB behind that of coherent antipodal CSK as predicted in Section VI-A.

3) Conclusion: The noise performance of chaotic switching can be maximized by choosing orthonormal basis functions. In the limit, chaotic switching can match the performance of coherent FSK. To reach this limit, a coherent DCSK receiver must be used. However, coherent DCSK can be implemented only if the basis functions are available at the receiver. To date, error-free recovery of chaotic basis functions, independently of the modulation, from the received noisy and distorted signal is not possible. Therefore, robust coherent chaotic modulation schemes have not yet been demonstrated successfully in practice.

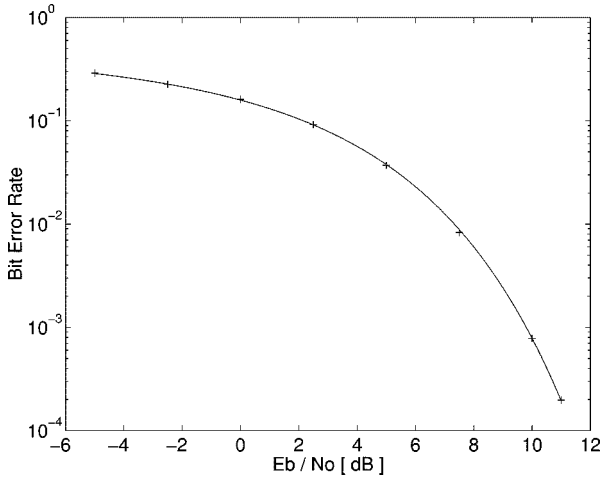

Fig. 14. Simulated ("+" marks) and theoretical (solid curve) noise performances of chaotic switching with two orthonormal basis functions. This figure is also valid for coherent DCSK which provides orthonormal basis functions.

4) Differentially Coherent Correlation Receiver for DCSK: Although coherent DCSK can in principle achieve the noise performance of coherent FSK, this level of performance can be reached only if the two basis functions $g_1(t)$ and $g_2(t)$ are available at the receiver and if they are orthonormal.

If the recovery of chaotic basis functions is not possible, then the special structure of the DCSK basis functions—each consists of a piece of chaotic waveform followed by a noninverted or inverted copy of itself—can be exploited to perform the demodulation. The differentially coherent DCSK demodulator [15] makes its decision by evaluating the correlation between the reference and information-bearing chips.

In a binary differentially coherent DCSK receiver, the reference signal $y(t)$ is the filtered noisy received signal, delayed by half a bit period. Note that different sample functions of filtered noise corrupt the two inputs of the correlator.

The observation signal is defined by

$$z_m = \int_{T/2}^{T} [\tilde{s}_m(t) + \tilde{n}(t)][\tilde{s}_m(t - T/2) + \tilde{n}(t - T/2)]\, dt. \quad (10)$$

If the time-varying channel varies slowly compared to the symbol rate, then the received and filtered DCSK signal is given by

$$\tilde{s}_m(t) = \begin{cases} \tilde{c}(t), & 0 \leq t < T/2, \\ (-1)^{m+1} \tilde{c}(t - T/2), & T/2 \leq t < T \end{cases} \quad (11)$$

where $\tilde{c}(\cdot)$ is the filtered version of $c(\cdot)$.

At best, $\tilde{c}(t) = c(t)$. Substituting (11) into (10), the observation signal becomes

$$\begin{aligned} z_m =& (-1)^{m+1} \int_{T/2}^{T} c^2(t - T/2)\, dt \\ &+ \int_{T/2}^{T} \tilde{n}(t) c(t - T/2)\, dt \\ &+ (-1)^{m+1} \int_{T/2}^{T} c(t - T/2) \tilde{n}(t - T/2)\, dt \\ &+ \int_{T/2}^{T} \tilde{n}(t) \tilde{n}(t - T/2)\, dt \end{aligned} \tag{12}$$

where $\tilde{n}(t)$ and $\tilde{n}(t - T/2)$ denote the sample functions of filtered noise that corrupt the reference and information-bearing parts of the received signal, respectively.

Assume that E_b is kept constant. Then $\int_{T/2}^{T} c^2(t - T/2)\, dt = E_b/2$ and the first term in (12) is equal to $\pm E_b/2$. The second, third, and fourth terms, which represent the contributions of the filtered channel noise, are zero-mean random variables. Therefore, the receiver is an *unbiased estimator* in this case; the optimum threshold level of the decision circuit is always zero, i.e., it is independent of the SNR.

Although the fourth term in (12) has zero mean, it has a non-Gaussian distribution. Due to this fourth term, the distribution of the observation signal is not Gaussian and its variance increases with the bit duration T and the bandwidth of the channel filter $2B$. Consequently, the noise performance of chaotic switching with two DCSK basis functions and a differentially coherent receiver decreases with either increasing bit duration or filter bandwidth [49]; this is illustrated in Fig. 15. Recall that this problem also appears in the case of noncoherent COOK.

5) Theoretical Noise Performance of Differentially Coherent DCSK: The exact analytical expression for the noise performance of differentially coherent DCSK was reported in [50]

$$\text{BER} = \frac{1}{2^{BT}} \exp\left(-\frac{E_b}{2N_0}\right) \times \sum_{i=0}^{BT-1} \frac{\left(\frac{E_b}{2N_0}\right)^i}{i!} \sum_{j=i}^{BT-1} \times \frac{1}{2^j} \binom{j + BT - 1}{j - i}. \tag{13}$$

The details of the development of this exact formula are given in [24]. Approximate expressions for the noise performance of CSK and DCSK using stochastic techniques can be found in [21] and [22].

To achieve this noise performance, the transmitted energy per bit must be kept constant [51]. This result shows that the noise performance of differentially coherent DCSK depends on both the bit duration T and the RF bandwidth $2B$ of the channel filter.

Equation (13) also shows that, for $BT = 1$, the noise performance of differentially coherent DCSK is as good as that of noncoherent binary FSK. Of course, in this case the DCSK signal becomes a narrow-band signal and the superior multipath performance of DCSK (see Section VIII) cannot be exploited.

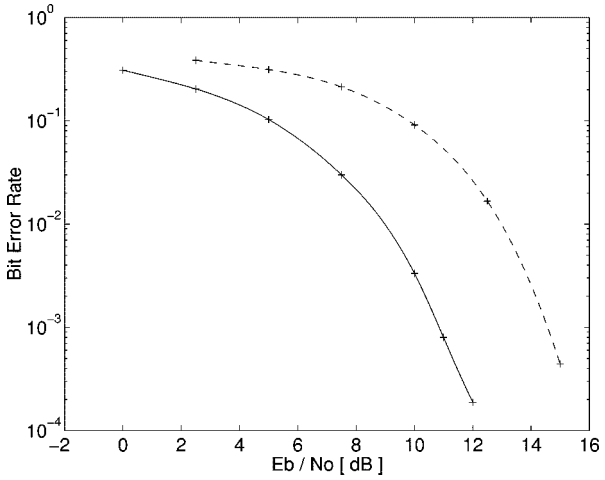

Fig. 15. Simulated noise performance of binary chaotic switching with DCSK basis functions and a differentially coherent receiver with short ($BT = 1$, solid curve) and long ($BT = 17$, dashed curve) bit durations.

Fig. 16 shows the effect of bit duration on the noise performance of differentially coherent DCSK, where the RF bandwidth is 17 MHz and (from left to right) the bit durations are 1, 2, 4, and 8 μs. The solid curves show the analytical predictions from (13), while the results of simulations are denoted by "+" marks.

The effect of RF bandwidth on the noise performance is shown in Fig. 17, where the bit duration is 2 μs and, from left to right, the RF channel bandwidths are 8, 12, and 17 MHz. Note that increasing the RF bandwidth decreases the noise performance of the system; however, it simultaneously improves the multipath performance (see Section VIII).

6) Conclusion: Given two basis functions and a noncoherent correlation receiver, the best noise performance can be achieved by chaotic switching with orthonormal DCSK basis functions and a differentially coherent receiver.

VII. Comparison of Noise Performance and Feasibility of Chaotic Modulation Schemes

In Sections V and VI, we have considered the noise performance of CSK with one and two basis functions.

The best possible noise performance curves for antipodal CSK modulation with coherent demodulation, COOK with noncoherent demodulation, chaotic switching with orthonormal basis functions and coherent demodulation, and chaotic switching with DCSK basis functions and a differentially coherent receiver are summarized in Fig. 18, where $BT = 1$ for the noncoherent COOK and differentially coherent DCSK. The noise performance curves for BPSK and coherent FSK are also shown, for comparison.

In the case of a single basis function, if one can recover this basis function *exactly* at the receiver, then the noise performance of antipodal CSK can theoretically reach that of BPSK. This is the best possible noise performance that could be achieved by any digital modulation scheme over an AWGN channel.

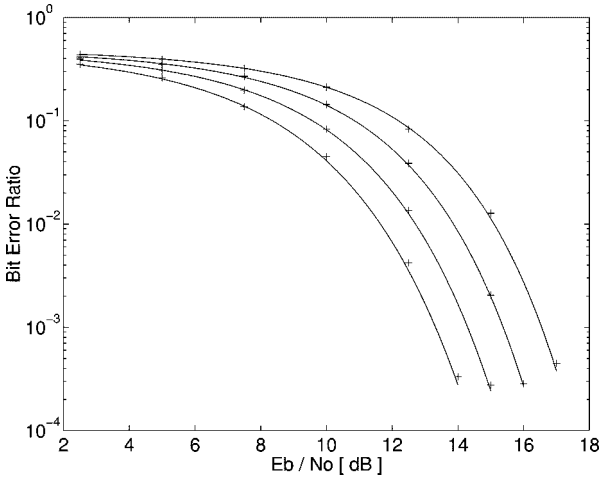

Fig. 16. Effect of bit duration on the noise performance of differentially coherent DCSK. From left to right the bit durations are 1, 2, 4 and 8 μs.

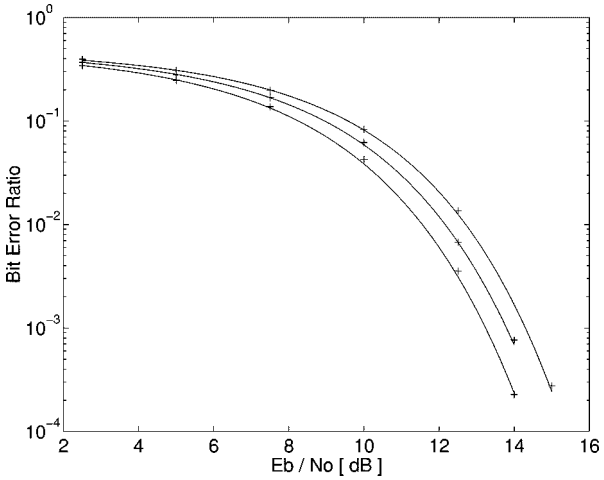

Fig. 17. Effect of RF channel bandwidth on the noise performance of differentially coherent DCSK. From left to right, the RF channel bandwidths are 8, 12, and 17 MHz.

In order to reach this level of performance, the chaotic basis function must be recovered independently of the modulation; we are not aware of any receiver structure in the literature that can do this in a sufficiently robust manner.

If the basis function cannot be recovered independently of the modulation, then COOK offers the best noise performance for the single-basis function case. The disadvantages of COOK are that the dynamic range of the transmitted power level varies between zero and twice the average transmitted power level and that the optimum decision threshold at the receiver depends on the SNR.

Chaotic switching offers a two-basis function modulation scheme where the average power level of the transmitted signal can be kept constant and the decision threshold at the receiver is independent of the SNR. The noise performance of chaotic switching with coherent detection can reach that of coherent FSK, provided that orthonormal basis functions are used. In particular, chaotic switching with DCSK basis functions can reach the performance of coherent FSK if the basis functions can be regenerated at the receiver.

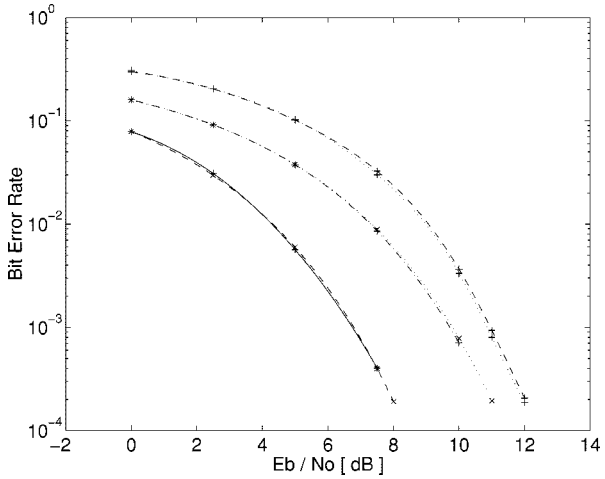

Fig. 18. Simulated optimum noise performance of antipodal CSK modulation with coherent demodulation [solid curve with "+" marks (left)], COOK with noncoherent demodulation [dashed curve with "+" marks (right)], chaotic switching with orthonormal basis functions and coherent demodulation [dash-dot curve with "+" marks (center)], and chaotic switching with DCSK basis functions and a differentially coherent receiver [dotted curve with "$\circ$" marks (right)]. The noise performance curves for BPSK [dashed curve with "$\circ$" marks (left)] and coherent FSK [dotted curve with "$\times$" marks (center)] are also shown, for comparison.

If the basis functions cannot be recovered, a DCSK transmission can be demodulated using a differentially coherent receiver. The noise performance of this chaotic communications system is at most 3 dB worse than that of DPSK with autocorrelation demodulation [36].

The same conclusion was drawn in [24], where the waveform communication concept was extended to correlator-based chaotic communications schemes. The paper showed that the shapes of chaotic basis functions, which are different for each transmitted symbol, have no effect on the noise performance, provided that orthonormal basis functions are used.

VIII. Multipath Performance

In many applications such as wireless local area networks (WLAN) and indoor radio, the received signal contains components which have traveled from the transmitter to the receiver via multiple propagation paths with differing delays; this phenomenon is called *multipath propagation* [37], [52].

Components arriving via different propagation paths may add destructively, resulting in deep frequency-selective fading. Conventional narrow-band systems fail catastrophically if a *multipath-related null*, defined below, coincides with the carrier frequency.

In the applications mentioned above, the distance between the transmitter and the receiver is relatively small; hence, the attenuation of the telecommunications channel is moderate. The effect which limits the performance of communications in such an environment is not the additive channel (thermal) noise N_0 but deep frequency-selective fading caused by multipath propagation. In these applications, the most important system parameter is the sensitivity to multipath.

In Sections V and VI, we have concluded that the noise performance of differentially coherent DCSK, even with constant energy per bit, in a single-ray AWGN channel is worse than that of coherent conventional narrow-band modulation schemes. However, DCSK has potentially lower sensitivity to multipath, because:

1) the demodulation is performed without carrier synchronization;
2) the transmitted signal is a wide-band signal which cannot be completely canceled by a multipath-related null.

Since differentially coherent FM-DCSK offers a simple system configuration and the best noise performance when the chaotic basis functions cannot be recovered at the receiver, we present computer simulations of its multipath performance in this section. Following the IEEE 802.11 WLAN standard [53], we set the RF channel bandwidth to 17 MHz. To illustrate the wide-band property of chaotic modulations schemes, the spectrum of an FM-DCSK system designed for WLAN application is shown in Fig. 19 [54]. The center frequency of the FM-DCSK modulator is 36 MHz, the data rate is 500 kbit/s, and the channel allocation corresponds to the IEEE 802.11 WLAN standard. The transmitter contains a mixer circuit to transpose the modulator output into the 2.4-GHz ISM band and a bandpass filter to suppress the unwanted skirt.

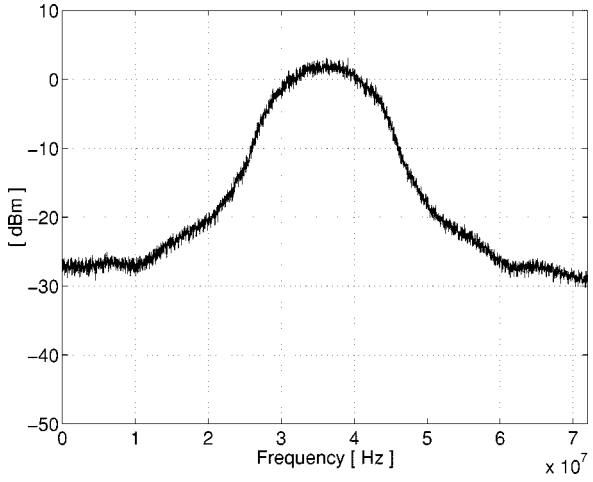

Fig. 19. Output spectrum of an FM-DCSK system. The bit duration is 2 μs and the RF channel bandwidth is 17 MHz.

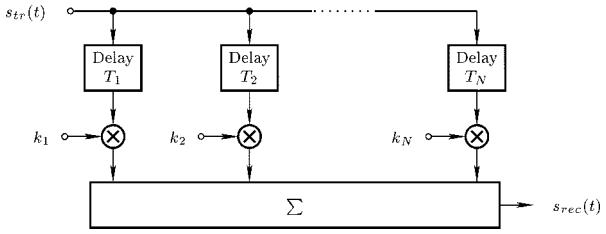

Fig. 20. Tapped delay line model of an RF multipath radio channel.

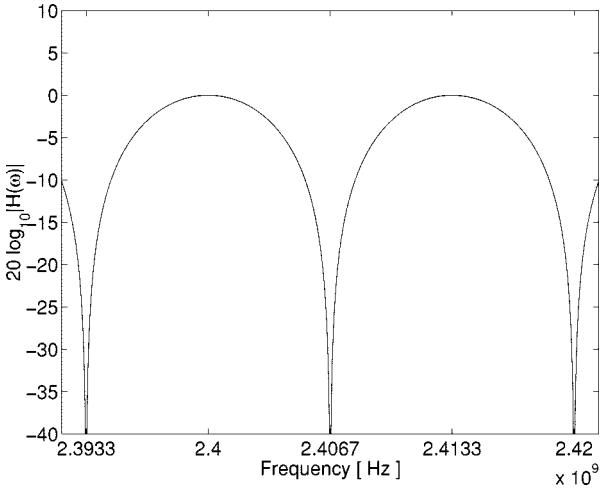

Fig. 21. Magnitude response of a two-ray multipath channel for $\Delta\tau = 75$ ns, which is typical in indoor office application.

A. Model of Multipath Channel

The tapped delay line model of a time-invariant multipath radio channel having N propagation paths is shown in Fig. 20. The radiated power is split and travels along the N paths, each of which is characterized by a delay T_l and gain k_l, where $l = 1, 2, \ldots, N$.

If a narrow-band telecommunications system is considered, then in the worst case two paths exist and the two received signals cancel each other completely at the carrier frequency ω_c, i.e.,

$$\Delta\tau\omega_c = (2n+1)\pi, \qquad n = 0, 1, 2, 3, \ldots$$

where $\Delta\tau = T_2 - T_1$ denotes the excess delay of the second path.

Let the two-ray multipath channel be characterized by its frequency response shown in Fig. 21. Note that the multipath-related nulls, where the attenuation becomes infinitely large, appear at

$$f_{null} = \frac{2n+1}{2\Delta\tau}, \qquad n = 0, 1, 2, 3\ldots. \tag{14}$$

Let the bandwidth of fading be defined as the frequency range over which the attenuation of the multipath channel is greater than 10 dB. Then the RF bandwidth of multipath fading can be expressed as

$$\Delta f_{null} \approx \frac{0.2}{\Delta\tau}. \tag{15}$$

Equations (14) and (15) show that the center frequencies of the multipath-related nulls, the distances between them, and their bandwidths, are determined by $\Delta\tau$; a shorter excess delay accentuates the problem.

Fig. 21 shows qualitatively why conventional narrow-band systems can fail catastrophically to operate over a multipath channel. Due to high attenuation appearing about the multipath-related nulls, the SNR becomes extremely low at the input of the receiver if the carrier frequency coincides with a multipath-related null. Consequently, the demodulator cannot operate. The situation becomes even worse if a carrier recovery circuit is used because a typical carrier recovery circuit such as a phase-locked loop cannot synchronize with

the carrier unless the input signal level exceeds a certain threshold.

In a chaotic modulation scheme, the power of the radiated signal is spread over a wide frequency range. The appearance of a multipath-related null means that part of the transmitted power is lost but the system still operates. Of course, the lower SNR at the input of the demodulator results in a worse BER. The special feature of DCSK that it does not use carrier synchronization to perform the demodulation makes it even more robust against multipath.

B. Quantitative Behavior of the FM-DCSK in PCS JTC Channels

The PCS Joint Technical Committee has recommended a comprehensive multipath channel model to check and compare the performance of personal communications and mobile telecommunications systems in both indoor and outdoor applications [55]. In indoor applications, considered here, channel models have been developed for office, residential, and commercial areas.

Each channel profile is characterized by the tapped delay line model shown in Fig. 20. To describe the various propagation conditions, three different channel profiles are given for each area. To model continuously varying propagation conditions, each channel profile is used, with probabilities determined by the JTC channel model.

This model assumes that the channel profile and the channel attenuation are correlated and it provides a statistical procedure for selecting the channel profiles as a function of attenuation. As a rule of thumb, we may say that if the channel attenuation is relatively low (below 50 dB, for example), then the simplest multipath channel model must be considered; this causes the smallest degradation in BER. Higher channel attenuation implies a more complex multipath channel model. For example, if the channel attenuation goes beyond 100 dB, then the most complex channel model causing the highest performance loss has to be considered.

Since different channel profiles are used to describe the propagation conditions in office, residential, and commercial areas, the simplest and most complex multipath channel models are different for each area.

In this section, we show by computer simulation the multipath performance of differentially coherent FM-DCSK for the simplest and most complex channel models. More details on multipath channel models will not be given here; we refer the interested reader to [55].

The number and frequencies of the multipath-related nulls appearing in the frequency response of the radio channel and their positions relative to the FM-DCSK center frequency are determined by the parameters of the multipath channel. In a real application, these parameters are varying continuously, thus changing the frequencies of the multipath-related nulls. To quantify this effect, but using the same multipath channel for every simulation, the parameters of the multipath channel models are kept constant but the center frequency of the FM-DCSK signal is varied. According to the IEEE 802.11 standard, we assume that the FM-DCSK system operates in the 2.4-GHz ISM band, and that $BT = 17$.

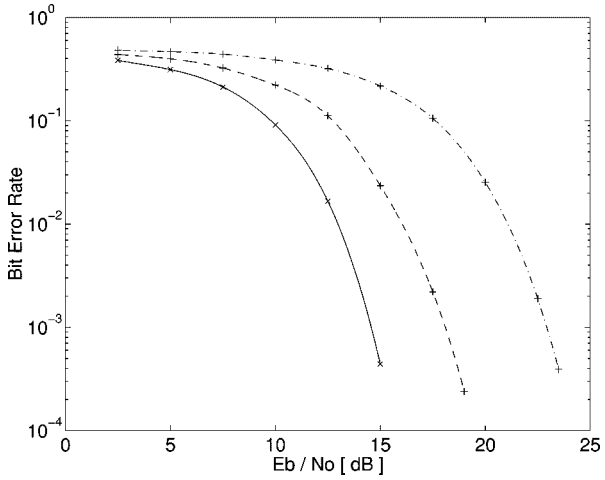

Fig. 22. FM-DCSK performance degradation in the indoor office application if the channel attenuation is less than 60 dB. The dashed and dash-dot curves show the best and worst results when the FM-DCSK center frequency is varied. For comparison, the noise performance without multipath (solid curve with "×" marks) is also plotted.

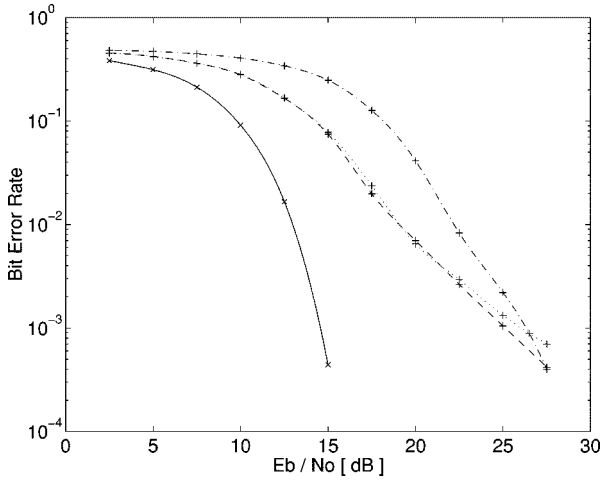

Fig. 23. Worst-case performance degradation in an FM-DCSK system when the channel attenuation exceeds 100 dB in the indoor office application. The dashed, dash-dot, and dotted curves correspond to different FM-DCSK center frequencies. For comparison, the noise performance without multipath (solid curve with "×" marks) is also plotted.

1) Performance Degradation in Office Area: FM-DCSK communications systems are potentially suitable for applications in indoor office areas, for example, to implement wireless local area networks. In these applications, if the attenuation of the radio channel is less than 60 dB, then the simplest JTC channel model has to be used. The FM-DCSK performance degradation in this case is shown in Fig. 22, where the dashed and dash-dot curves show the best and worst results, respectively, as the FM-DCSK center frequency is varied. The average loss in system performance is only 5.4 dB at $\mathrm{BER} = 10^{-3}$.

In the worst case, the attenuation of the radio channel exceeds 100 dB and the most complex multipath channel model must be considered. The performance degradation of an FM-DCSK system in this environment is shown in

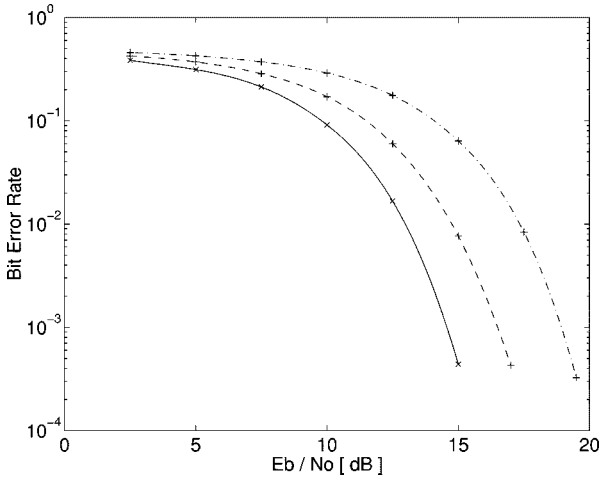

Fig. 24. FM-DCSK performance degradation in the indoor residential area when the channel attenuation is less than 50 dB. The dashed and dash-dot curves show the best and worst results when the FM-DCSK center frequency is varied. For comparison, the noise performance without multipath (solid curve with "×" marks) is also plotted.

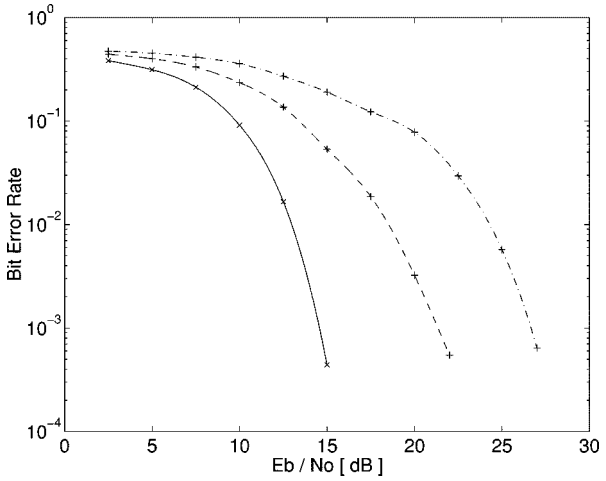

Fig. 25. Worst-case performance degradation in an FM-DCSK system when the channel attenuation exceeds 75 dB in the indoor residential area. The dashed and dash-dot curves show the best and worst results when the FM-DCSK center frequency is varied. For comparison, the noise performance without multipath (solid curve with "×" marks) is also plotted.

Fig. 23, where the dashed, dash-dot, and dotted curves correspond to different FM-DCSK center frequencies: 2.4, 2.41, and 2.42 GHz, respectively. Note that the average loss in system performance is only 11.2 dB at $\mathrm{BER} = 10^{-3}$, even in this worst-case situation.

2) Performance Degradation in Residential Area: The indoor residential area is another possible application environment for FM-DCSK communications systems. When the channel attenuation is less than 50 dB in this area, then the simplest channel model has to be used. The performance degradation of an FM-DCSK system under these propagation conditions is shown in Fig. 24, where the dashed and dash-dot curves show the best and worst results, respectively, as the FM-DCSK center frequency is varied.

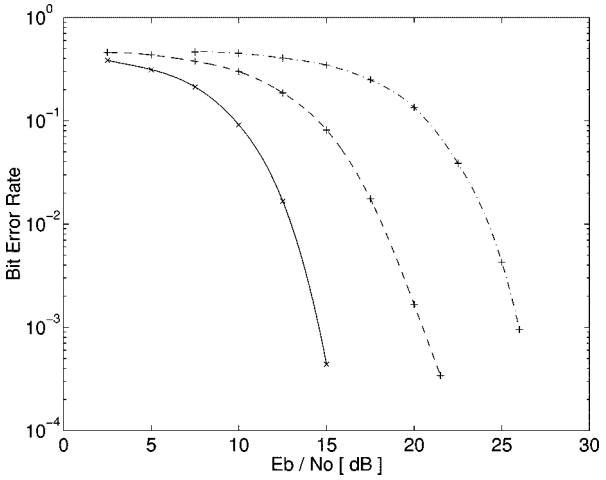

Fig. 26. FM-DCSK performance degradation in the indoor commercial application if the channel attenuation is less than 60 dB. The dashed and dash-dot curves show the best and worst results when the FM-DCSK center frequency is varied. For comparison, the noise performance without multipath (solid curve with "×" marks) is also plotted.

The average loss in system performance is only 3.1 dB at $\mathrm{BER} = 10^{-3}$.

The most complex model has to be considered when the channel attenuation goes beyond 75 dB. The performance degradation in this environment is shown in Fig. 25, where the dashed and dash-dot curves give the best and worst noise performance as the FM-DCSK center frequency is varied. The average loss in system performance is only 10.5 dB at $\mathrm{BER} = 10^{-3}$, even in this worst-case situation.

3) Performance Degradation in Commercial Area: The third potential application environment for FM-DCSK for which a JTC channel model has been developed is the indoor commercial area. In this application, if the attenuation of the radio channel is less than 60 dB, then the simplest channel model has to be used. The FM-DCSK performance degradation for this case is shown in Fig. 26, where the dashed and dash-dot curves show the best and worst results, respectively, as the FM-DCSK center frequency is varied. The average loss in system performance is 8.6 dB at $\mathrm{BER} = 10^{-3}$.

In the worst case, the attenuation of the radio channel exceeds 100 dB. The performance degradation of an FM-DCSK system in this environment is shown in Fig. 27, where the dashed and dash-dot curves show the best and worst result as the FM-DCSK center frequency is varied. The average loss in system performance is 11.0 dB at $\mathrm{BER} = 10^{-3}$ in this worst-case situation.

IX. Multiple Access Capable DCSK System

The autocorrelation function of a chaotic signal decays very rapidly and becomes almost zero even for relatively short delays. The cross correlation between chaotic signals resulting from different initial conditions or generated by different attractors is very low. These properties have been exploited in [29] and [30] to develop a multiuser-capable DCSK system.

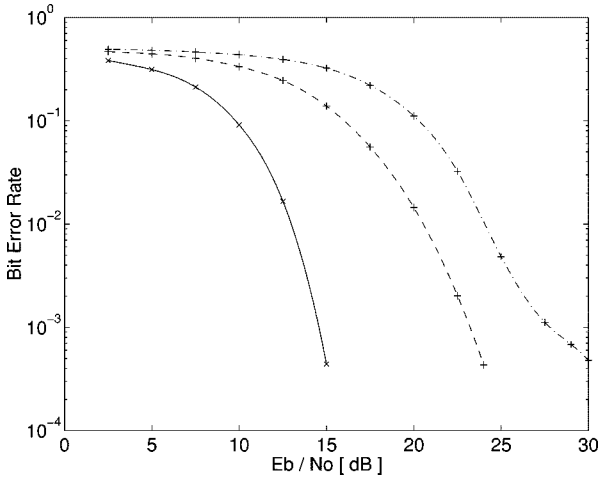

Fig. 27. Performance degradation in an FM-DCSK system when the channel attenuation exceeds 100 dB in the indoor commercial application. The dashed and dash-dot curves show the best and worst results when the FM-DCSK center frequency is varied. For comparison, the noise performance without multipath (solid curve with "×" marks) is also plotted.

However, simulations [29] have shown that chaotic signals having finite length are not orthogonal; this results in a high level of interference among radio channels. The source of interference is the cross correlation estimation problem which was discussed in Section III-B. This interference allows one to accommodate only a few users and to implement a low-quality communications channel. For example, for three users and a bit duration of 2 μs, the attainable BER has a lower bound of about 10^{-2}, even in the noise-free case.

To obtain two orthogonal DCSK basis functions, a chaotic signal was combined with the first two Walsh functions [40] in Section III-B. This technique can be extended for larger signal sets. For example, by means of the first N Walsh functions one may generate N orthogonal signals, thereby accommodating $N/2$ orthogonal binary telecommunication channels in the same frequency band. Since orthogonality is ensured by using Walsh functions, interference among the different users is zero provided that all Walsh functions are synchronized.

A. Model of the Multiuser Radio Channel

A model of a multiuser environment containing two FM-DCSK transceivers is shown in Fig. 28. The physical media that carry the signals from the transmitters to the receivers are represented by "Channel$_{XY}$," where $X \in 1, 2$ and $Y \in 1, 2$. The additive white Gaussian channel noise is modeled by $n_Y(t)$.

B. Application of Walsh Functions to Generate Orthogonal Basis Functions

First the elements of the orthonormal signal set have to be developed. Constant energy per bit is ensured by FM modulation, as shown in Fig. 5.

Let $u = 1, 2, \ldots, N/2$ and $j = 1, 2, \ldots, N$ denote the numbers of users and basis functions, respectively. Assume that $N/2 = 4$ binary communications channels have to be accommodated. To obtain eight orthogonal basis functions, the bit period has to be divided into $N = 8$ time slots and the first $N = 8$ Walsh functions have to be used, as shown in Fig. 29.

In the first time slot, an FM modulated chaotic signal $y_u(t)$ is transmitted for user u, i.e., $y_1(t)$, $y_2(t)$, $y_3(t)$, and $y_4(t)$ are transmitted for users 1, 2, 3, and 4, respectively, where $y_u(t)$ differs from zero for $0 \le t \le T/N$. Then these signals or their inverted copies are sent in the remaining seven time slots. The sign of the jth basis function segment transmitted in the kth time slot is chosen according to the jth Walsh function w_j, as shown in Fig. 29. Let $g_{j,k}(t)$, $k = 1, 2, \ldots, N$ denote the segment of the jth basis function transmitted in the kth time slot. Then

$$g_{j,k}(t) = w_{j,k} y_u(t) \tag{16}$$

where the kth element of w_j is given by $w_{j,k}$.

In this way, we have developed eight orthonormal basis functions: $g_j(t)$, $j = 1, 2, \ldots, 8$; each transmitter uses two of these to transmit information bits "0" and "1." For example, user 1 maps bits "1" and "0" to $g_1(t)$ and to $g_2(t)$, respectively.

Although only four users (the first eight Walsh functions) are considered in this section, the method presented here can be extended to an arbitrary, but limited number of users. However, a large number of users degrades the spectral properties of the transmitted signal.

C. Multiuser Capable FM-DCSK Demodulator

The received signal $r_u(t)$ of the uth user contains the sum of all the transmitted signals $s_1(t)$, $s_2(t)$, $\ldots s_{N/2}(t)$ and additive white Gaussian noise $n_u(t)$. To demodulate the received signal at the uth receiver, first the signal $y_u(t)$ transmitted in the first time slot by the uth transmitter is recovered from the noisy received signal and then the two basis functions $g_{2u-1}(t)$ and $g_{2u}(t)$ of the uth channel are reconstructed. Having reconstructed the two basis functions, a coherent correlation receiver, shown in Fig. 13, is used for the demodulation, i.e., the two reconstructed DCSK basis functions are correlated with the received noisy signal $r_u(t)$ and the decision is made in favor of the larger correlator output.

Let us determine the two correlator outputs for receiver 1. Assume that all users are synchronized and let $r_{1,k}(t)$ denote the signal received by the first receiver in the kth time slot.

To estimate $y_1(t)$, each segment of the received signal has to be multiplied by the Walsh function belonging to the basis function to be recovered. Assume first that bit "1" has been sent by transmitter 1. To reconstruct the first basis function $g_1(t)$, each segment of $r_{1,k}(t)$ has to be multiplied by 1 according to the first Walsh function. The estimate of $y_1(t)$ is obtained as

$$\begin{aligned}\hat{y}_1^{(11)}(t) &= \frac{1}{N}\sum_{k=1}^{N} w_{1,k} r_{1,k}(t) = \frac{1}{N}\sum_{k=1}^{N} r_{1,k}(t) \\ &= \frac{1}{N}\sum_{k=1}^{N}\left[n_{1,k}(t) + \sum_{u=1}^{N/2} s_{u,k}(t)\right]\end{aligned} \tag{17}$$

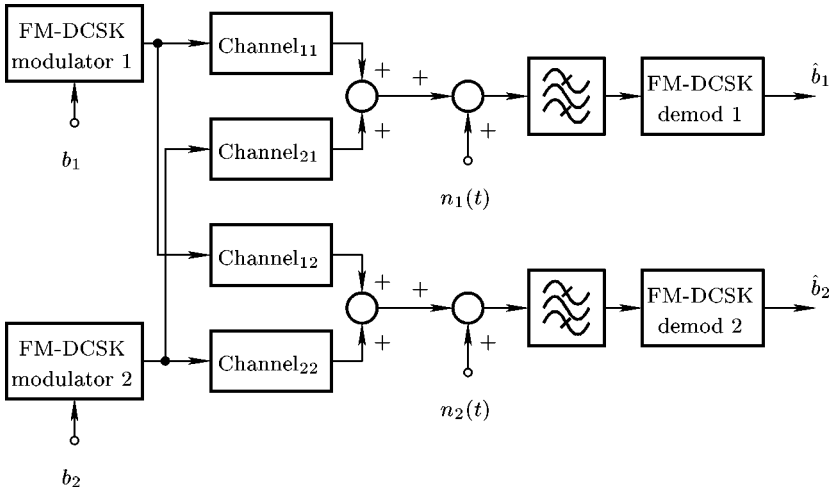

Fig. 28. Block diagram of a two-user FM-DCSK system.

where $s_{u,k}(t)$ is the segment of the signal of uth user transmitted in kth time slot. The signal $s_{u,k}(t)$ is equal to $g_{2u,k}(t)$ or $g_{2u-1,k}(t)$ depending on the bit transmitted by uth user. It follows from the orthogonality of the Walsh functions that

$$\frac{1}{N}\sum_{k=1}^{N} g_{j,k}(t) = \begin{cases} y_1(t), & \text{if } j=1 \\ 0, & \text{elsewhere.} \end{cases} \tag{18}$$

Substituting (18) into (17), we get the estimate of $y_1(t)$

$$\hat{y}_1^{(11)}(t) = y_1(t) + \frac{1}{N}\sum_{k=1}^{N} n_{1,k}(t). \tag{19}$$

For the noise-free case, $\hat{y}_1^{(11)}(t) = y_1(t)$.

The first receiver is also recovering an estimate of $y_1(t)$ based on the assumption that bit "0," i.e., the second basis function, has been transmitted. Since the second Walsh function is 1 for $k = 1, \ldots, 4$ and -1 for $k = 5, \ldots, 8$, the estimate of $y_1(t)$ is obtained as

$$\begin{aligned}\hat{y}_1^{(12)}(t) &= \frac{1}{N}\sum_{k=1}^{N} w_{2,k} r_{1,k}(t) \\ &= \frac{1}{N}\left[\sum_{k=1}^{N/2} r_{1,k}(t) - \sum_{k=N/2+1}^{N} r_{1,k}(t)\right] \\ &= \frac{1}{N}\left(\sum_{k=1}^{N/2}\left[\sum_{u=1}^{N/2} s_{u,k}(t) + n_{1,k}(t)\right]\right. \\ &\quad \left. - \sum_{k=N/2+1}^{N}\left[\sum_{u=1}^{N/2} s_{u,k}(t) + n_{1,k}(t)\right]\right). \end{aligned} \tag{20}$$

Exploiting again that $s_{u,k}(t)$ is equal to $g_{2u,k}(t)$ or $g_{2u-1,k}(t)$ and substituting (18) into (20), the estimate of $y_1(t)$ for this case is obtained as

$$\hat{y}_1^{(12)}(t) = \frac{1}{N}\left[\sum_{k=1}^{N/2} n_{1,k}(t) - \sum_{k=N/2+1}^{N} n_{1,k}(t)\right] \tag{21}$$

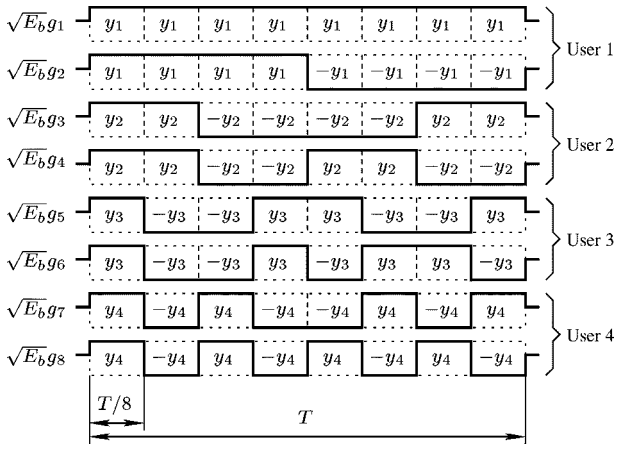

Fig. 29. Segmentation of the transmitted signals using Walsh functions for a four-user application. To get a compact figure, the time dependence of the analog signals is not shown explicitly.

For the noise-free case, $\hat{y}_1^{(12)}(t) = 0$.

From (19) and (21), receiver 1 regenerates the estimates of $g_1(t)$ and $g_2(t)$ using the first and second Walsh functions, respectively, and determines the elements of the observation vector

$$z_{1j} = \int_0^T r(t)\hat{g}_j(t)\,dt \tag{22}$$

where $j = 1, 2$ and $\hat{g}_j(t)$ denotes the estimate of the jth basis function. For the noise-free case, i.e., for perfect recovery of basis function, (22) reduces to

$$z_{11} = \sqrt{E_b}, \quad \text{and} \quad z_{12} = 0. \tag{23}$$

When transmitter 1 sends bit "0," $g_2(t)$ is radiated. Using the technique discussed above for bit "1," the elements of the observation vector are obtained for the noise-free case as

$$z_{21} = 0, \quad \text{and} \quad z_{22} = \sqrt{E_b}. \tag{24}$$

Finally, the decision at receiver 1 is made by comparing z_{j1} with z_{j2}, as shown in Fig. 13.

Inspecting (19) and (20), two important conclusions can be drawn.

1) Due to the orthogonality of the Walsh functions, there is no interference between different users.
2) The effect of channel noise is reduced due to averaging. This averaging improves the noise performance of each FM-DCSK radio channel.

For the other users, estimates of the basis functions $\hat{g}_j(t)$, $j = 3, \ldots, N$ are recovered in the same manner; the only difference is that in estimating $y_u(t)$ and regenerating $\hat{g}_j(t)$, the jth Walsh function must be used.

D. Performance Evaluation

The system performance of a multiuser-capable FM-DCSK system with a bit duration of $T = 2$ μs and total RF bandwidth of $2B = 17$ MHz has been evaluated by computer simulation for the case when a maximum of four users can be accommodated, i.e., when $N = 8$.

Fig. 30 shows the noise performance when one (dashed curve), three (dash-dot curve) and four (solid curve) users are communicating over the same radio channel simultaneously. The unused channels were switched off during the simulation.

Fig. 30 shows that the noise performance is almost independent of the number of users. This property follows from the orthogonality of the Walsh functions which results in complete cancellation of the signals transmitted by the other users in each demodulator.

The noise performance of a single-user FM-DCSK system having the same system parameters was given in Fig. 17. Comparison of Figs. 17 and 30 shows that the noise performance of the multiuser-capable FM-DCSK system is better than that of the single-user one. The reason is that the transmitted signal has a modified structure and a different demodulation strategy is used to recover the transmitted information. The price of better noise performance is a slight degradation in the spectral properties of the radiated FM-DCSK signal and a tighter specification for the clock recovery circuit because all users must be synchronized at the symbol level.

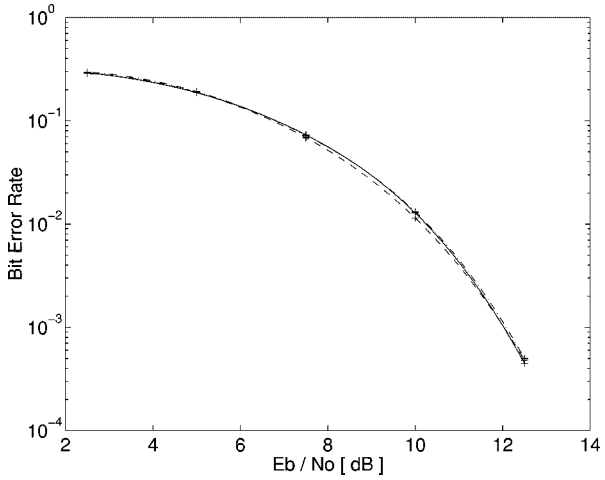

Fig. 30. Noise performance of a multiuser-capable FM-DCSK system for $N = 8$ when one (dashed curve), two (dash-dot curve) and four (solid curve) users are communicating over the channel. The maximum number of users is $N/2 = 4$.

X. Enhanced Versions of the DCSK System

In DCSK, half of the energy per bit is lost because the reference chip only provides the reference signal for the demodulator and does not carry any information. This loss is reduced in the simplest version of enhanced DCSK (DCSK/S), where the reference chip is followed by $K > 1$ information bearing chips [32]. For example, when $K = 4$, $2B = 17$ MHz and $T = 2$ μs, the noise performance of FM-DCSK/S at $\mathrm{BER} = 10^{-3}$ can be improved by 1.4 dB. This improvement results from sending four information bits with the same reference.

Depending on the information bit to be transmitted, the information-bearing chips are copies or inverted copies of the reference chip. In the original DCSK and DCSK/S receivers, the decision is made by determining the correlations between the information-bearing chips and the reference. However, note that additional information can be gained from the correlations between the information-bearing chips. In the most sophisticated versions of enhanced DCSK systems, the correlation between every pair of chips is evaluated at the receiver and this extra information is used to improve the noise performance.

Let $\tilde{r}_k(t) = \tilde{r}\left(t - ((k-1)/(K+1))T\right)$, $k = 1, 2, \ldots, (K+1)$, denote the signal received in the kth time slot, where $\tilde{r}_1(t)$ is the reference and $\tilde{r}_k(t)$, $2 \leq k \leq (K+1)$, are the information-bearing chips. Let E_S denote the energy per chip. The correlation between the kth and lth chips is given by

$$z_{k,l} = \tilde{r}_k(t) \star \tilde{r}_l(t) = \int_0^{T/(K+1)} \tilde{r}_k(t)\tilde{r}_l(t)\,dt.$$

There are at least three ways to exploit the additional correlations in enhanced DCSK in order to improve its noise performance: enhanced DCSK with noise reduction by averaging (DCSK/AV) [56], enhanced DCSK with nonredundant "error correction" using the shortest path algorithm (DCSK/SP), and enhanced DCSK with nonredundant "error correction" using the spanning tree algorithm (DCSK/ST) [57].

A. Analysis of the Correlations Between the Received Chips

The redundancy carried by the enhanced DCSK signal can be exploited if a measure of goodness for each correlation can be found.

Let the probability of sending bits "1" and "0" be 0.5 and consider the correlation between the kth and lth chips. Fig. 31 shows the histograms of $z_{k,l} = \tilde{r}_k(t) \star \tilde{r}_l(t)$. Note that in the region near the origin, the probability of making a wrong or correct decision is almost the same; the low absolute value of the correlation implies a high probability of a wrong decision.

In the original DCSK and DCSK/S, only the signs of the correlations between chips are used in making a decision. However, the absolute value of each correlation is a measure of probability of making a correct decision. In particular, this measure is used as a weighting factor in DCSK/AV, DCSK/SP, and DCSK/ST.

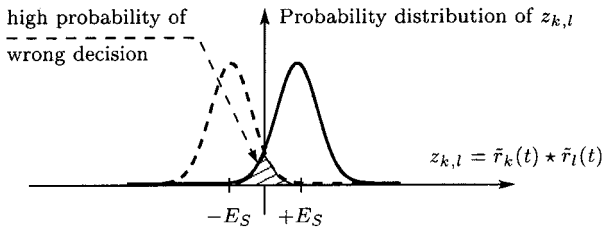

Fig. 31. Probability distribution of the correlation between the kth and lth chips.

In DCSK/AV, the modulation is removed and the reference chip is regenerated as a weighted average of the received reference and information-bearing chips. The weights are selected so that the effects of noisy chips are suppressed [56]. Using this technique, an improvement of 2.7 dB can be achieved when $K = 4$, $2B = 17$ MHz and $T = 2$ μs.

In DCSK/SP and DCSK/ST, the correlations are calculated for each pair of chips and the probability of a wrong decision is minimized using the absolute values of these correlations. Both of these techniques use optimum graph search algorithms to determine the best decision strategy. They yield similar improvements in noise performance. For brevity, we discuss only DCSK/ST in detail. The performances of DCSK/AV and DCSK/SP are included in Section X-C for comparison.

B. Application of the Minimum Cost Spanning Tree Algorithm to Improve the DCSK Noise Performance

The decision procedure is illustrated by the graph shown in Fig. 32, where the vertices of the graph represent all received chips, including the reference one, and the edges connecting the vertices represent the correlations between pairs of chips. It follows from the special structure of the enhanced DCSK signal that the decision for each bit can be made along any path in the graph which starts from $k = 1$ and terminates at the desired chip.

To minimize the required computational effort, the decision has to be made using the minimum number of edges. Note that K edges are required to recover the K bits. The subgraph, which connects all the $K + 1$ vertices and contains only K edges, is called a spanning tree.

The *minimum cost spanning tree* algorithm [58] is used to select the spanning tree which offers the minimum probability of wrong decisions for the K bits. In this approach, each edge of the graph shown in Fig. 32 is characterized by a weight, and each spanning tree is characterized by a cost which is the sum of these weights. The algorithm selects the tree which has the minimum cost.

To minimize the BER, the weights associated with each edge must have a high value if the probability of a wrong decision is high, and a low one in the opposite case. Recall that the absolute value of the correlation characterizes the probability of a wrong decision, i.e., the weight for the edge connecting the kth and lth vertices can be defined as

$$w_{k,l} = \frac{1}{|\tilde{r}_k(t) \star \tilde{r}_l(t)| + \epsilon}$$

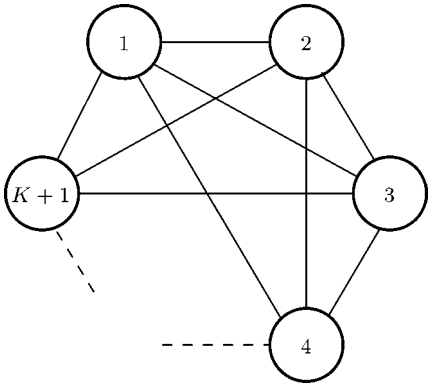

Fig. 32. Graph showing all possible decision paths for an enhanced DCSK signal having one reference and K information-bearing chips. The vertices represent the received chips while the edges give the correlations between pairs of chips.

where ϵ is a small positive number whose function is to prevent division by zero. As shown in Fig. 31, a large weight is associated with each edge for which the probability of a wrong decision is high.

The steps of the enhanced DCSK technique are as follows:

1) each reference chip is followed by K information-bearing chips, i.e., instead of individual bits, K-bit symbols are transmitted in one block;
2) the correlations between all pairs of received chips are calculated;
3) the weights associated with all edges are determined;
4) using the minimum cost spanning tree algorithm, the spanning tree which offers the lowest probability of a wrong decision is selected for the K unknown bits;
5) the decision is made for each bit using the edges of the corresponding spanning tree.

C. Performance Evaluation

To compare the effectiveness of the different techniques, the noise performances of enhanced DCSK systems were evaluated by computer simulation for the following system parameters: $2B = 17$ MHz, $T = 2$ μs, and $K = 4$.

The noise performance of the DCSK/S, DCSK/AV, DCSK/ST, and DCSK/SP is shown in Fig. 33. Recall that in DCSK/S one reference chip is used to transmit K information chips and no further processing is performed. In the other cases, the additional techniques described above are used in order to improve the noise performance of the system.

The highest improvements in noise performance are achieved by applying the shortest path and the minimum cost spanning tree algorithms. Note that these two methods yield almost identical improvements in noise performance. An improvement of 3.4 dB can be achieved at $\mathrm{BER} = 10^{-3}$, as shown in Fig. 33.

The costs of higher noise performance and data rate are:

1) a more complex system configuration;
2) degradation in the spectral properties of the radiated signal;
3) higher sensitivity to time-varying channels.

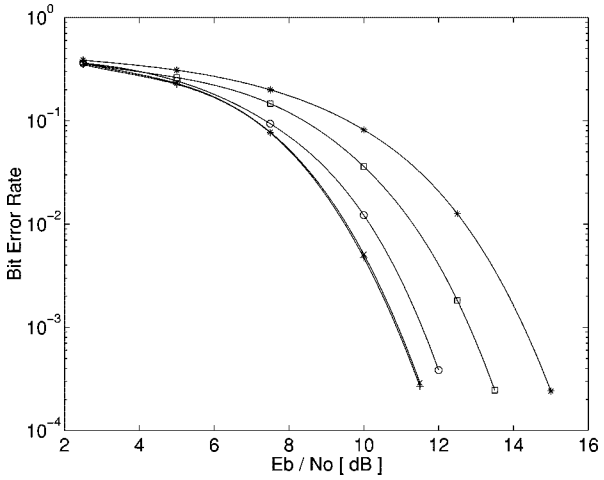

Fig. 33. Noise performance of the different enhanced DCSK systems. The curves for DCSK/SP, DCSK/ST, DCSK/AV, and DCSK/S are represented by "+," "×," "∘," and "□" marks, respectively. Note that the noise performance of DCSK/SP and DCSK/ST is almost the same. The noise performance of the original DCSK system (solid curve with "∗" marks) is shown for comparison.

XI. Conclusion

In chaotic modulation schemes, the transmitted signal is a wide-band signal. The objectives of using a wide-band signal as the carrier are twofold:

1) to overcome the multipath propagation problem;
2) to reduce the transmitted power spectral density in order to reduce the interference caused in adjacent radio communications channels.

Of the chaotic modulation schemes published to date, DCSK with orthonormal basis functions, also referred in the literature as FM-DCSK [16], offers the best robustness against multipath and channel imperfections.

It is frequently asked whether chaotic modulation schemes can offer any advantages over conventional narrow-band systems. If the propagation conditions are so good that the basis function(s) can be regenerated at the receiver, then digital modulation schemes using conventional orthonormal (typically periodic[5]) basis functions, and orthonormal chaotic basis functions can achieve similar levels of noise performance, as discussed in Sections V and VI, and shown theoretically in [24].

The main question from an implementation perspective is the ease with which the basis functions can be regenerated.

We believe that it is fundamentally easier to regenerate a periodic basis function than a chaotic one. We conjecture, therefore, that the noise performance of digital chaotic modulation with coherent correlation receivers will always lag behind that of equivalent modulation schemes using periodic basis functions.

[5]The application of noise as a carrier for digital communications system was proposed in [59]. A system configuration for the qualitatively similar FM-DCSK system was described in [60]. The novelty of the latter solution over the former is that the estimation problem has been recognized and solved, and the chaos generator provides a bounded, more robust and simpler source of nonperiodic basis functions.

If the propagation conditions are such that coherent detection is impossible, then chaotic switching with orthonormal DCSK basis functions and a differentially coherent receiver (DCSK, for short), offers the best possible performance for a chaotic digital modulation scheme. In the limit, the noise performance of DCSK lags at most 3 dB behind that of DPSK with autocorrelation demodulation [36], [50].

In this case, the choice of periodic or chaotic basis functions is determined by the propagation conditions. In particular, the multipath performance of a DCSK system can be improved by increasing the transmission bandwidth.

Another important issue is interference. If the operating environment is such that interference with other narrow-band radio systems working in the same frequency band should be minimized, then a spread spectrum system must be used; this can be implemented using chaotic basis functions, where the chaotic waveform is the spreading signal. For a fixed transmitted power, the wider the bandwidth of the chaotic signal, the lower the interference caused.

Although signal spreading in a chaotic communications scheme reduces the interfering signal level for narrow-band systems sharing the same frequency band, the converse is not necessarily true. Interference to a chaotic communications system caused by other users in the same band can be suppressed only by using coherent demodulation techniques.

We stress that, although we have discussed the noise performance bounds for chaotic modulation schemes in the context of the limits for conventional narrow-band modulation techniques, the comparison is not fair in the sense that chaotic modulation is intended for use as an inherently wide-band communications system. Although it performs worse than conventional narrow-band modulation schemes in a simple AWGN channel, the advantage of DCSK is that the fall-off in its performance in a multipath channel is more gradual than that of an equivalent narrow-band modulation scheme.

This result is highlighted dramatically in Fig. 34, where the performance degradation in a narrow-band DPSK system ($BT = 1$; classical DPSK with the optimum receiver configuration, referred as to "optimum DPSK" [36]) is compared with that of a wide-band differentially coherent FM-DCSK ($BT = 17$) system. The bit duration was set to 2 μs in both cases and the RF bandwidth of the DCSK signal was 17 MHz. The solid and dashed curves give the noise performance of optimum DPSK and FM-DCSK, respectively, over a single-ray AWGN channel.

The noise performance of these modulation schemes was evaluated over a two-ray multipath channel characterized by $\Delta\tau = 100$ ns and $k_1 = k_2 = 0.5$. The excess delay of 100 ns is typical of WLAN applications in large warehouses.

Recall that there is no need for carrier recovery in optimum DPSK receivers [36]. We assumed in the simulations that the carrier frequency is known exactly at the DPSK receiver; a frequency error, if present, results in a performance degradation in both the single-ray and multipath channels. Although the single-ray performance of differentially coherent FM-DCSK is worse than that of DPSK, its multipath performance is significantly better, despite the fact that the carrier

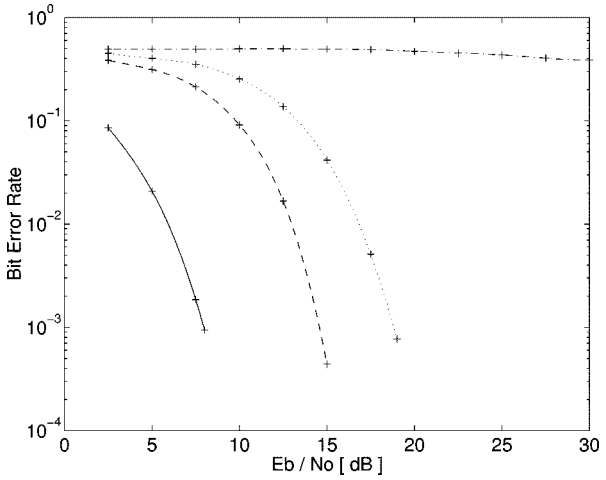

Fig. 34. Simulated noise performance curves for optimum DPSK and wide-band FM-DCSK in a single-ray channel (solid and dashed, respectively) and in a two-ray multipath channel (dash-dot and dotted, respectively). While FM-DCSK disimproves by about 4 dB, DPSK fails completely.

Table 1
Performance Degradation of an FM-DCSK System Over the Multipath Channels Elaborated by the PCS Joint Technical Committee. Performance Losses are Given for the Simplest (Low Attenuation) and Most Complex (Very High Attenuation) Cases

Area	Simplest model	Worst-case model
Office	5.4 dB	11.2 dB
Residential	3.1 dB	10.5 dB
Commercial	8.6 dB	11.0 dB

recovery problem which would accentuate the problem further does not appear in optimum DPSK.

Therefore, FM-DCSK offers a performance advantage over conventional communications schemes in multipath environments when the propagation conditions are so poor that coherent detection or detection of DPSK with an optimum receiver configuration is not possible.

This conclusion was confirmed in Section VIII, where the multipath performance of DCSK was evaluated using the comprehensive indoor multipath channel models developed by the PCS Joint Technical Committee. The results of these simulations are summarized in Table 1 for the indoor office, residential, and commercial applications. These results confirm our conjecture in 1997 [17] that the DCSK modulation scheme could outperform conventional narrow-band modulation schemes under poor propagation conditions.

In many applications, at least a limited multiple-access capability has to be offered. Chaotic sample functions having finite length are not orthogonal; this is why orthogonal signal sets and channels cannot be developed directly from chaotic signals.

We showed in Section IX that an orthogonal signal set, and consequently orthogonal telecommunications channels, can be developed by combining a chaotic signal with Walsh functions. In this way, FM-DCSK may accommodate a limited number of users. However, too great a number of users would result in a very complex system configuration.

The noise performance of FM-DCSK lags behind that of suboptimum DPSK. The noise performance of FM-DCSK can be improved by a few decibels, for example, the application of the minimum cost tree algorithm results in a 3.4 dB improvement, as was shown in Section X. The price of this improvement is a more complex receiver configuration.

REFERENCES

[1] L. M. Pecora and T. L. Carroll, "Synchronization in chaotic systems," *Phys. Rev. Lett.*, vol. 64, no. 8, pp. 821–824, 1990.

[2] K. M. Cuomo, A. V. Oppenheim, and S. H. Strogatz, "Robustness and signal recovery in a synchronized chaotic system," *Int. J. Bif. Chaos*, vol. 3, pp. 1629–1638, Dec. 1993.

[3] K. M. Cuomo and A. V. Oppenheim, "Circuit implementation of synchronized chaos with applications to communications," *Phys. Rev. Lett.*, vol. 71, pp. 65–68, July 1993.

[4] L. Kocarev and U. Parlitz, "General approach for chaotic synchronization with applications to communication," *Phys. Rev. Lett.*, vol. 74, pp. 5028–5031, June 19, 1995.

[5] H. Papadopoulos, G. W. Wornell, and A. V. Oppenheim, "Maximum likelihood estimation of a class of chaotic signals," *IEEE Trans. Inform. Theory*, vol. 41, pp. 312–317, Jan. 1995.

[6] J. Kawata, Y. Nishio, H. Dedieu, and A. Ushida, "Performance comparison of communication systems using chaos synchronization," *IEICE Trans. Fund.*, vol. E82-A, pp. 1322–1328, July 1999.

[7] U. Parlitz, L. O. Chua, L. Kocarev, K. S. Halle, and A. Shang, "Transmission of digital signals by chaotic synchronization," *Int. J. Bif. Chaos*, vol. 2, pp. 973–977, 1992.

[8] H. Dedieu, M. P. Kennedy, and M. Hasler, "Chaos shift keying: Modulation and demodulation of a chaotic carrier using self-synchronizing Chua's circuits," *IEEE Trans. Circuits Syst. II (Special Issue on Chaos in Nonlinear Electronic Circuits—Part C: Applications)*, vol. 40, pp. 634–642, Oct. 1993.

[9] C. W. Wu and L. O. Chua, "Transmission of digital signals by chaotic synchronization," *Int. J. Bif. Chaos*, vol. 3, no. 6, pp. 1619–1627, 1993.

[10] S. Hayes, C. Grebogi, and E. Ott, "Communicating with chaos," *Phys. Rev. Lett.*, vol. 70, pp. 3031–3034, May 1993.

[11] J. Schweizer and M. P. Kennedy, "Predictive Poincaré control," *Phys. Rev. E*, vol. 52, pp. 4865–4876, Nov. 1995.

[12] U. Feldmann, M. Hasler, and W. Schwarz, "Communication by chaotic signals: The inverse system approach," *Int. J. Circuit Theory Appl.*, vol. 24, pp. 551–579, 1996.

[13] T. Yang, "Recovery of digital signals from chaotic switching," *Int. J. Circuit Theory Appl.*, vol. 23, no. 6, pp. 611–615, 1995.

[14] M. Hasler, "Engineering chaos for secure communication systems," *Phil. Trans. R. Soc. Lond.*, vol. 353, no. 1710, pp. 115–126, 1995.

[15] G. Kolumbán, B. Vizvári, W. Schwarz, and A. Abel, "Differential chaos shift keying: A robust coding for chaotic communication," in *Proc. NDES'96*, Seville, Spain, June 27–28, 1996, pp. 87–92.

[16] G. Kolumbán, G. Kis, Z. Jákó, and M. P. Kennedy, "FM-DCSK: A robust modulation scheme for chaotic communications," *IEICE Trans. Fund.*, vol. E81-A, pp. 1798–1802, Oct. 1998.

[17] G. Kolumbán, M. P. Kennedy, and L. O. Chua, "The role of synchronization in digital communications using chaos—Part I: Fundamentals of digital communications," *IEEE Trans. Circuits Syst. I*, vol. 44, pp. 927–936, Oct. 1997.

[18] ——, "The role of synchronization in digital communication using chaos—Part II: Chaotic modulation and chaotic synchronization," *IEEE Trans. Circuits Syst. I*, vol. 45, pp. 1129–1140, Nov. 1998.

[19] G. Kolumbán and M. P. Kennedy, "The role of synchronization in digital communication using chaos—Part III: Performance bounds for correlation receivers," *IEEE Trans. Circuits Syst. I*, vol. 47, pp. 1673–1683, Dec. 2000.

[20] A. Abel, M. Götz, and W. Schwarz, "Statistical analysis of chaotic communication schemes," in *Proc. IEEE—ISCAS'98*, vol. IV, Monterey, CA, May 31–June 3, 1998, pp. 465–468.

[21] A. Abel, W. Schwarz, and M. Götz, "Noise performance of chaotic communication systems," *IEEE Trans. Circuits Syst. I*, vol. 47, pp. 1726–1732, Dec. 2000.

[22] M. Sushchik, L. Tsimring, and A. Volkovskii, "Performance analysis of correlation-based communication schemes utilizing chaos," *IEEE Trans. Circuits Syst. I*, vol. 47, pp. 1684–1691, Dec. 2000.
[23] W. Schwarz, M. Götz, K. Kelber, A. Abel, T. Falk, and F. Dachselt, "Statistical analysis and design of chaotic systems," in *Chaotic Electronics in Telecommunications*, M. P. Kennedy, R. Rovatti, and G. Setti, Eds. Boca Raton, FL: CRC, 2000.
[24] G. Kolumbán, "Theoretical noise performance of correlator-based chaotic communications schemes," *IEEE Trans. Circuits Syst. I*, vol. 47, pp. 1692–1701, Dec. 2000.
[25] M. P. Kennedy and G. Kolumbán, Guest, Eds., "Special issue on noncoherent chaotic communications," in *IEEE Trans. Circuits Syst. I*, Dec. 2000, vol. 47.
[26] M. P. Kennedy, R. Rovatti, and G. Setti, Eds., *Chaotic Electronics in Telecommunications*. Boca Raton, FL: CRC, 2000.
[27] K. Król, L. Azzinnari, E. Korpela, A. Mozsàry, M. Talonen, and V. Porra, "An experimental FM-DCSK chaos radio system," in *Proc. ECCTD'01*, Espoo, Finland, Aug. 28–31, 2001, pp. III-17–III-20.
[28] M. P. Kennedy, G. Kolumbán, G. Kis, and Z. Jákó, "Performance evaluation of FM-DCSK modulation in multipath environments," *IEEE Trans. Circuits Syst. I*, vol. 47, pp. 1702–1711, Dec. 2000.
[29] Z. Jákó, G. Kis, and G. Kolumbán, "Multiple access capability of the FM-DCSK chaotic communications system," in *Proc. NDES'2000*, Catania, Italy, May 18–20, 2000, pp. 52–55.
[30] F. C. M. Lau, M. M. Yip, C. K. Tse, and S. F. Hau, "A multiple access technique for differential chaos shift keying," in *Proc. IEEE—ISCAS'2001*, vol. III, Sydney, Australia, May 6–9, 2001, pp. 317–320.
[31] G. M. Maggio and O. D. Feo, "T-CSK: A robust approach to chaos-based communications," in *Proc. NDES'2000*, Catania, Italy, May 18–20, 2000, pp. 37–41.
[32] Z. Jákó, "Performance improvement of DCSK modulation," in *Proc. NDES'98*, Budapest, Hungary, July 16–18, 1998, pp. 119–122.
[33] J. Schweizer, "The performance of chaos shift keying: Synchronization versus symbolic backtracking," in *Proc. IEEE—ISCAS'98*, vol. IV, Monterey, CA, May 31–June 3, 1998, pp. 469–472.
[34] T. Schimming, H. Dedieu, M. Hasler, and M. Ogorzalek, "Noise filtering in chaos-based communication," in *Chaotic Electronics in Telecommunications*, M. P. Kennedy, R. Rovatti, and G. Setti, Eds. Boca Raton, FL: CRC, 2000, pp. 221–252.
[35] M. Hasler, "Ergodic chaos shift keying," in *Proc. IEEE—ISCAS'01*, vol. III, Sydney, Australia, May 6–9, 2001, pp. 145–148.
[36] M. K. Simon, S. H. Hinedi, and W. C. Lindsey, *Digital Communication Techniques: Signal Design and Detection*. Englewood Cliffs, NJ: Prentice-Hall, 1995.
[37] S. Haykin, *Communication Systems*, 3rd ed. New York: Wiley, 1994.
[38] M. P. Kennedy and G. Kolumbán, "Digital communications using chaos," *Signal Process.*, vol. 80, pp. 1307–1320, July 2000.
[39] J. S. Bendat and A. G. Piersol, *Measurement and Analysis of Random Data*. New York: Wiley, 1966.
[40] S. Tzafestas, *Walsh Functions in Signal and Systems Analysis and Design*. New York: Van Nostrand Reinhold, 1985.
[41] G. Kis, Z. Jákó, M. P. Kennedy, and G. Kolumbán, "Chaotic communications without synchronization," in *Proc. 6th IEE Conf. Telecommunications*, Edinburgh, U.K., Mar. 29–Apr. 1, 1998, pp. 49–53.
[42] G. Kolumbán, "Basis function description of chaotic modulation schemes," in *Proc. NDES'2000*, Catania, Italy, May 18–20, 2000, pp. 165–169.
[43] G. Kis and G. Baldwin, "Efficient FM-DCSK radio system simulator," in *Proc. ECCTD'99*, Stresa, Italy, Aug. 29–Sept. 2, 1999, pp. 884–887.
[44] Y. G. Hong, H. S. Qin, and G. Chen, "Adaptive synchronization of chaotic systems via state or output feedback control," *Int. J. Bif. Chaos*, vol. 11, pp. 1149–1158, Apr. 2001.
[45] Q. Xie, G. Chen, and E. M. Bollt, "Hybrid chaos synchronization and its application in information processing," *Math. Comput. Model.*, 2001.
[46] M. E. Yalçin, J. A. K. Suykens, and J. Vandewalle, "Master–slave synchronization of Lur'e systems with time delay," *Int. J. Bif. Chaos*, vol. 11, pp. 1707–1722, June 2001.
[47] G. Millerioux and C. Mira, "Finite-time global chaos synchronization for piecewise linear maps," *IEEE Trans. Circuits Syst. I*, vol. 48, pp. 111–116, Jan. 2001.
[48] C. C. Chen and K. Yao, "Stochastic calculus based numerical evaluation and performance analysis of chaotic communication systems," *IEEE Trans. Circuits Syst. I*, vol. 47, pp. 1663–1672, Dec. 2000.
[49] A. Abel, M. Götz, and W. Schwarz, "DCSK and DPSK—What makes them different?," in *Proc. NOLTA'98*, vol. I, Crans Montana, Switzerland, Sept. 14–17, 1998, pp. 67–72.
[50] G. Kolumbán and M. P. Kennedy, "DCSK: Chaotic modulation for multipath environments," in *Presymp. Tutorial IEEE-ISCAS'2000*, May 28, 2000.
[51] G. Kolumbán, "Exact analytical expression for the noise performance of FM-DCSK," in *Proc. NOLTA'2000*, Dresden, Germany, Sept. 17–21, 2000, pp. 735–738.
[52] R. C. Dixon, *Spread Spectrum Systems With Commercial Applications*, 3rd ed. New York: Wiley, 1994.
[53] S. Jost and C. Palmer. (1998) New standards and radio chipset solutions enable untethered information systems: *PRISM*™ 2.4GHz 'Antenna-to-bits' IEEE 802.11 DSSS radio chipset solution. Intersil Corporation, Tech. Rep. [Online]. Available: http://www.intersil.com/design/prism/papers/
[54] M. P. Kennedy, G. Kolumbán, and G. Kis, "Chaotic modulation for robust digital communications over multipath channels," *Int. J. Bif. Chaos*, vol. 10, no. 4, pp. 695–718, 2000.
[55] K. Pahlavan and A. H. Levesque, *Wireless Information Networks*. New York: Wiley, 1995.
[56] G. Kolumbán, Z. Jákó, and M. P. Kennedy, "Enhanced versions of DCSK and FM-DCSK data transmission systems," in *Proc. IEEE—ISCAS'99*, vol. IV, Orlando, FL, May 30–June 2, 1999, pp. 475–478.
[57] Z. Jákó, D. Fournier-Prunaret, V. Guglielmi, and G. Kis, "Non-redundant error correction in FM-DCSK chaotic communications systems," in *Proc. ECCTD'01*, vol. II, Espoo, Finland, Aug. 28–31 2001, pp. 193–196.
[58] E. Kreyszig, *Advanced Engineering Mathematics*. New York: Wiley, 1999.
[59] W. R. Ramsay and J. J. J. Spilker, "Binary digital communication system," U.S. Patent S4 363 130, Dec. 7, 1982.
[60] M. P. Kennedy, G. Kolumbán, G. Kis, and Z. Jákó, "Binary digital communication system using a chaotic frequency-modulated carrier," Irish Patent S80913, Nov. 28, 1997.

Géza Kolumbán (Senior Member, IEEE) received the M.S. and Ph.D. degrees from the Technical University of Budapest and the C.Sc. degree from the Hungarian Academy of Sciences in 1976, 1990, and 1990 respectively.

After graduation, he was employed as a research engineer by the Fine Mechanical Enterprise, Hungary, where he developed local generators, microwave transistor power amplifiers, and VCO circuits for high-capacity microwave analog radio relay systems. He joined the Research Institute for Telecommunications, Hungary, in 1980, where he was involved in many system engineering projects such as SCPC-type satellite telecommunications system, microwave satellite up- and down-converters, low-capacity microwave digital radio system, etc. He headed a group of engineers, whose duty was to develop frequency synthesizers and local generators for frequency hopping spread spectrum and satellite systems. He spent one year with Bilkent University in Turkey (1991–1992) and another year with the Eastern Mediterranean University in Cyprus (1992–1993) as an Associate Professor. He returned to the Budapest University of Technology and Economics (called Technical University of Budapest before 2000) in 1993, where he is an Associate Professor at the Department of Measurement and Information Systems. He has been a visiting researcher to the Electronics Research Laboratory, University of California at Berkeley, University College Dublin and Cork, EPFL, Switzerland, and TU Dresden, Germany. His current research and professional interests include nonlinear dynamics of different-type phase-locked loops, frequency synthesis by sampling phase-locked loop, mixed signal processing, computer simulation of complex systems, chaotic communications, and applications of chaotic signals in measurement engineering.

Michael Peter Kennedy (Fellow, IEEE) received the B.E. (electronics) degree from the National University of Ireland in 1984, and was awarded the M.S. and Ph.D. degrees by the University of California at Berkeley in 1987 and 1991, respectively, for his contributions to the study of neural networks and nonlinear dynamics.

He worked as a Design Engineer with Philips Electronics, a Postdoctoral Research Engineer at the Electronics Research Laboratory, University of California at Berkeley, and as a Professeur Invité at the EPFL, Switzerland. From 1992 to 1999, he was on the faculty of the Department of Electronic and Electrical Engineering at University College Dublin (UCD), where he taught Electronic Circuits and Computer-Aided Circuit Analysis, and directed the undergraduate Electronics laboratory. In 1999, he joined University College Cork as Professor and Head of the Department of Microelectronic Engineering. He has published more than 200 articles in the area of nonlinear circuits, holds two patents, and has taught courses on nonlinear dynamics and chaos in England, Switzerland, Italy, and Hungary. His research interests are in the simulation, design, and analysis of nonlinear dynamical systems for applications in communications and signal processing.

He received the 1991 Best Paper Award from the International Journal of Circuit Theory and Applications and the Best Paper Award at the European Conference on Circuit Theory and Design 1999. He served as Associate Editor of the IEEE TRANSACTIONS ON CIRCUITS AND SYSTEMS from 1993 to 1995 and from 1999 to 2002. He received the IEEE Third Millennium Medal and the IEEE CAS Society Golden Jubilee Medal in 2000. In 2001, he was awarded the inaugural Parson's Medal for Engineering Sciences by the Royal Irish Academy.

Zoltán Jákó received the M.S. degree from the University "Transylvania" Brasov, Romania, in 1995. He is currently working toward the Ph.D. degree at the Department of Measurement and Information Systems of the Budapest University of Technology and Economics.

His current research interests include the chaotic behavior of analog phase-locked loop, cleaning noisy chaotic signals, and chaotic communications.

Gábor Kis received the M.S. degree from the Budapest University of Technology and Economics in 1997. He is currently working toward the Ph.D. degree at the Department of Measurement and Information Systems.

His research interests include chaotic behavior of the analog phase-locked loop, design and simulation of telecommunications systems, wireless communications systems, and chaotic communications.